Author comments in reply to the anonymous referee on "A tropospheric chemistry reanalysis for the years 2005–2012 based on an assimilation of OMI, MLS, TES and MOPITT satellite data" by K. Miyazaki et al.

We want to thank the referee for the helpful comments, and for his/her compliments on the work presented, the evaluation of the results and clarity of the text. At the same time we fully agree with the referee that the major challenge lies in "unraveling the reasons behind the changes observed" because many aspects of the model are optimised simultaneously in the assimilation process. We have revised the manuscript according to the comments, and hope that the revised version of the manuscript is now suitable for publication. Below are the referee comments in italics with our replies in normal font.

Reply to Referee #1

Overall, the results of the assimilation are quite encouraging. Nevertheless, unravelling the reason behind many of the observed changes proves challenging, given the tremendous number of degrees of freedom for an inversion such as this and the sheer volume of results to analyze. I wish there were more instances where the assimilation results could be translated directly into an improved understanding of some underlying deficiency in the model's transport, chemistry, or deposition. Further, there are a few areas where the inversion doesn't preform as well (such as for NO2 concentrations in polluted areas) or where the results just don't make sense (such as the inference of large increases in NOx and CO emissions in the US and Europe). The paper will be suitable for publication after the authors make revisions to address these and other comments provided below.

The revised manuscript more explicitly discusses the limitations of the current chemical reanalysis calculation, as described below.

Specific comments:

242: It seems a bit out of place to bring up advantages of this approach over another here. But if you want to discuss this, then it also seems a bit odd to only mention the advantages of one approach – surely there are disadvantages as well.

The sentence has been removed from the manuscript.

260: It might be clearer to say: Xb is the ith row (or column? I'm not sure) of an N × k matrix Xb,

where . . .

Corrected.

260: What is the size of N here? Is it just the size of the state vector (38), of the state vector times the physical system dimension?

The size of N is the state vector times the forecast model dimension, which is described in the revised manuscript as follow:
'... where N indicates the system dimension (the state vector size times the physical system dimension)'

Eqn 3: To be consistent with Eq (1), shouldn't it be Yib?

Corrected.

Section 2.2.1: Something is missing from this section, namely the application of the forecast model itself. Where does that come into play? Should it act on xb, or xa from the previous step?

The following sentence has been added to Section 2.2:
'The assimilation step transforms a background ensemble ($¥vec{x}_{i}^b; i=1,¥ldots, k$) into an analysis ensemble ($vec{x}_{i}^a; i=1,¥ldots, k$) and updates the analysis mean, where x represents the model variable, b the background state, a the analysis state, and k the ensemble size.'

The final sentence in Section 2.2.2 has been rewritten as follows:
'The new ensemble members x_i^b after the next forecast step are obtained from model simulations starting from the analysis ensemble x_i^a.'

Section 2.3: The explanation of the state vector is not clear. Line 300 implies that the following discussion pertains to both emission and concentration scaling, but then the description that follows on lines 302 - 304 is only for emissions scaling.

The sentence has been rewritten as:
'The chemical concentrations in the state vector are expressed in the form of volume mixing ratio, while the emissions are represented by scaling factors for each surface grid cell for the total NOx and CO emissions at the surface (not for individual sectors), and for each production rate profile of the LNOx

sources.'

Section 2.5: Why is the notation here for x and y different than other sections, where they are not italicized?

Corrected.

Section 2.7: I realize that inclusion of scaling factors in each surface grid cell for emissions and each grid cell for concentrations is made feasible through the localization step (otherwise the system dimension would be too big). Still, the details of how this is setup are not clear. Are different sets of ensembles used within each localization region, or are there only 30 ensemble members spanning the entire globe? If the latter, this seems like a tremendously large space to span by so few members. The scale L seems to be of order of a few grid cells in the horizontal. But CO emissions have an impact on concentrations several km away. How is the setting of L to only 600 km justified?

The observational information is localized in both the horizontal and vertical to avoid spurious long-range error correlations caused by the limited ensemble size. The localization scale (L) was optimized based on sensitivity experiments on the basis of comparisons with independent observations. L = 600 km corresponds to the cut-off radius of 2191 km (i.e. the localized area diameter of 4382 km), which enables us to assimilate remote observations. The ensemble spread is estimated at every model grid point based on the ensemble model forecast. The background error covariance varies with time and space, reflecting the dominant atmospheric processes and locations of the observations. The sentences have been rewritten as follows:

'The horizontal localization scale L was set to 450 km for NOx emissions and to 600 km for CO emissions, LNOx, and for the concentrations. The physical vertical localization length was set to ln(p1/p2) [hPa] = 0.2. These choices are based on sensitivity experiments (Miyazaki et al., 2012b), for which the influence of an observation was set to zero when the horizontal distance between the observation and analysis point was larger than $2L¥times¥sqrt{10/3}$ (e.g., the cut off radius is set to 2191 km for L = 600 km). We also account for the influence of the averaging kernels of the instruments, which captures the vertical sensitivity profiles of the retrievals. The ensemble members and ensemble spread (error covariance) do vary from one location to the next, and from one species to the next, thereby representing the large number of degrees of freedom contained in the model and they way these are constrained by the observations.'

593: Or this could indicate mis-specification of R?

Yes, there is a possibility that the observation error is not reasonably specified. The sentence has been rewritten as follows:

'For the OMI NO_2 assimilation, the $\chi 2$ is > 1, which indicates overconfidence in the model or underestimation of the super-observation error (computed as a combination of the measurement error and the representativeness error).'

604: This is a bit at odds with the figure and following sentence, which show that χ2 is not constant. Perhaps rephrase?

The sentences have been rewritten as follows:

'Before 2010, the annual mean $\chi 2$ is roughly constant, which confirms the good stability of the performance. Seasonal and interannual variations, especially after 2010, of $\chi 2$ can be attributed to variations in the coverage and quality of satellite retrievals as well as changes in atmospheric conditions (e.g., chemical lifetime and dominant transport type).'

701: One need not hypothesize about the information content of the TES data – the DOFs (trace of averaging kernel) will quantify this directly and could be used to check your explanation here.

The following sentence has been added:

'Jourdain et al. (2007) showed that the TES retrievals have 1-2 DOFs in the troposphere, with the largest DOFs for clear-sky scenes occurring at low latitudes where TES can distinguish between lower and upper tropospheric O_3.'

Section 4.3: One aspect that warrants discussion is the difference between the distribution of the analysis increment and the changes in OmF between the control run and reanalysis. Granted transport, chemistry, and the observation operator make these not correspond 1:1; however, I had a hard time rationalizing what I saw. For example, presumably much of the improvement in MLS ozone occurs in the upper troposphere. How is it that the OmF for MLS, which was mostly negative south of 50 S but positive and negative north of 50 N be improved by an increment that is positive nearly everywhere?

The OmF for MLS O_3 is shown for the vertical layer between 216 and 100 hPa in Fig. 2, whereas the analysis increment is shown for the vertical level at 200 hPa in Fig. 3. Because the ozone concentration increases rapidly with height at the altitudes, the OmF averaged between 216 hPa and 100 hPa is largely

different from that at 200 hPa, and does not show good correspondence to the analysis increment at 200 hPa. The analysis increment averaged between 200 and 100 hPa (as shown below) corresponds well to the OmF averaged between 216 and 100 hPa (Fig. 2 in the manuscript). To explain this, the following sentence has been added:

'The obtained analysis increments correspond well to the OmF in the control run at the same altitude (figure not shown), confirming that the data assimilation effectively reduced the model errors through the analysis steps.'

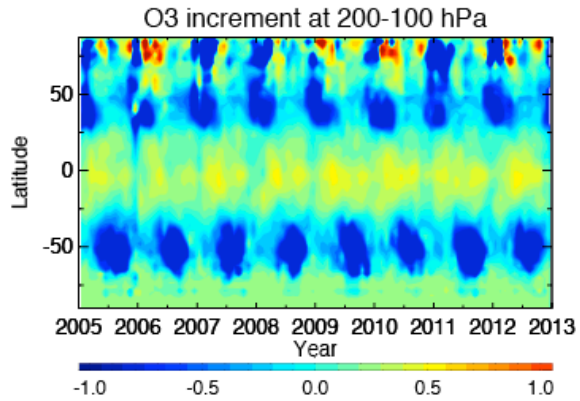

Figure: Time-latitude cross-section of the analysis increment obtained for O_3 between 200 and 100 hPa (in ppb/analysis step).

Also, line 717 implies that the drastic differences in ozone increments at different vertical levels is a sign that the system is working well. I would consider another possibility that the system is under-constrained, despite the results of the χ2 test, and that the increments are exhibiting high frequency oscillations that lie in null space of your forecast model (rather than the observation space). The χ2 test makes assumptions about the normality of the state parameters and observations, which may not hold.

There might be such a possibility. However, in all cases studied, we did not find any high-frequency oscillations in the obtained analysis increment. In data assimilation, those aspects of the system which are not constrained by the observations will stay close to the model forecast if the assimilation is working properly, and we should not expect spurious oscillations. This is similar to retrievals, where a-priori information will suppress null-space oscillations. If we observe clear analysis increments this usually is a good sign and means the assimilation is using the information from the observations to improve the OmA as compared to the OmF. Our results suggest that there is enough information to distinguish emission signatures from concentration biases.

Fig 7: Maybe something is mis-labeled, but I had a hard time following the description of this figure in the text, in comparison to looking at the figure itself, which seems to show pretty much no improvement

between the control and reanalysis for O3. This is further confused by the Table which is referenced describing the errors in ppb, while the text describes them in %, which makes it a bit hard to follow.

The first sentence of the second paragraph in Section 5.1.2 has been rewritten as follows:
'Although the improvement is not large in the upper troposphere (500-300 hPa, Fig. 7), an improved agreement with the MOZAIC/IAGOS measurements is found in the reanalysis run in the middle troposphere (850-500 hPa) and at the aircraft-cruising altitude (300-200 hPa), as summarised in Table~1.'

Because ozone concentration largely varies with height, we believe that it is useful to discuss the relative error (in %) in the main text.

Fig 9: I also found it difficult to identify in these figures the features described in the text. Please instead provide a plot of the model minus observation for the control and reanalysis results.

The model minus observation plots have been added in Figs. 9 and 13.

854: Is the author refering to other previous studies (if so, please cite them) or the present work?

The sentence has been rewritten as follows:
'These characteristics of the bias are commonly found in comparisons with global ozonesonde observations in this study (c.f., Section 5.1.1) and are reduced effectively in the reanalysis.'

879: however, the performance was significantly worse at the surface

The sentence has been rewritten as follows:
'The comparisons show improved agreements in the reanalysis for the middle and upper troposphere during INTEX-B over Mexico and during the ARCTAS campaign over the Arctic, but the model's positive bias near the surface is further increased for the INTEX-B profile.'

931: I'm not sure what is meant by "emissions constraints provided at the ground surface". Also, it's not clear why the improvements with respect to the IAGOS data are attributed to emissions rather than the adjustment of the concentrations directly.

In the reanalysis calculation, the CO concentrations were not adjusted by the data assimilation analysis.

Only the surface emissions were adjusted for CO in the data assimilation framework, as described in the manuscript. The sentence has been rewritten as follows:
'This confirms that the constraints provided for the surface emissions are propagated well into the concentrations of the entire troposphere with a delay in the peak timing and decay in the amplitude. Note that the CO concentrations were not directly adjusted in the data assimilation framework.'

971-977: This is interesting. I wish there were more analysis like this showing how careful analysis of the model performance can be used to parse errors in emissions from errors in concentrations.

We plan to conduct more detailed analyses in future studies to demonstrate the usefulness of the simultaneous concentration and emission optimization.

1052: I wonder to what extent the poorer performance for the NO2 concentrations in urban areas is owing to the adjustments made only to NOx and CO and not VOCs.

I agree that further constraints on wider fields could help to adjust the model chemical equilibrium state and to reduce the negative bias in the NO_2 concentrations. This is discussed in Section 8 as follows:

'For instance, the reanalysis still has large negative biases in NO_2 concentrations over the polluted regions, which may be associated with errors in for instance the model chemical equilibrium states, planetary boundary layer (PBL) mixing, and diurnal variations of chemical processes and emissions. Adjusting additional model parameters such as VOC emissions, deposition, and/or chemical reactions rates by adding observational constraints will help to reduce model errors.'

1055: This argument is a bit dangerous to make, since the perturbations from the model's natural dynamic chemical state are being forced by the state vector increments. So this would seem to be a potential pitfall of adjusting both concentrations and emissions simultaneously.

Indeed we agree that there is a danger of adjusting the concentration even though the emissions may be wrong, or, vice versa, correcting emissions to compensate for chemistry/transport errors. Concentration adjustments may quickly be lost in the PBL due to the short lifetime of NOx, while emission adjustments could be more efficient to store the information over longer time periods. The sentence has been reformulated as follows:
'There may be several reasons for the remaining underestimation of NO_2 concentrations. The analysis increment can partly be lost after the forecast because of the short lifetime of NOx (Miyazaki and Eskes

2013), especially when concentrations are adjusted. Other model processes, such as the diurnal cycle, boundary layer mixing and venting, and the chemical equilibrium at overpass may not be described well. Also, the averaging kernels show a relatively small sensitivity close to the surface, resulting in relatively smaller adjustments in the assimilation.'

1070: The impact of the observations at one hour of the day should be much longer reaching, given the substantial role of NOx on the chemical state. Despite the short lifetime of NO2 itself, this impact can be multiple days, reaching several hundred km.

There could be such longer time influences on NO_2 through the propagation of observational information in the complex chemical system, influencing species like ozone or reactive nitrogen reservoir species. Nevertheless, direct (and local) constraints are considered to be much more important in correcting tropospheric NO_2.

1172: It seems like if this still "remains an important issue" then you might find a more recent paper on the topic than 2003.

The following paper is cited in the revised manuscript:
Stone, D., Whalley, L. K., Heard, D. E.: Tropospheric OH and HO_2 radicals: field measurements and model comparisons.. *Chemical Society Reviews*, 41 (19), 6348-6404, 2012.

Section 6: Several studies have investigated trends in NO2 over the US and Europe in the past decade, with direct inferences for NOx emissions trends being largely negative (e.g., Russell et al., ACP, 2012). Unfortunately, the results don't look anything like the trends shown here with increasing NOx emissions. This is probably the weakest aspect of this paper, along with similar issues for the CO emission trends – how do you reconcile these results with known improvements in combustion efficiency / control technology in developed nations? This needs to be seriously addressed.

We agree with this comment and are very much interested in this topic. We have found that there were similar negative trends in the NO_2 concentrations over the eastern US for 2005-2011 between the OMI observations (-38 %) and the reanalysis (-35 %). The negative trend in the reanalysis is larger than that in the model simulation (-17 %) and is closer to the observational estimates, including the result of Russell et al. (2012) (-32 % for the same period but for a wider area). The estimated surface NOx emissions also showed a larger negative trend over the eastern US for 2005-2012, a larger positive trend over China for 2005-2010, and a larger negative trend over Europe for 2005-2010 in the reanalysis than in the a priori

emissions; the estimated emission trends in this study are similar to those in Tong et al. (2015), Castellanos and Boersma (2012), and Gu et al. (2013), respectively, for the same area/period. Although the mean concentration and the interannual variation of tropospheric NO_2 were generally underestimated in the reanalysis as discussed in the manuscript, the estimated emissions can be expected to provide implications for year-to-year emission variations. Because the main purpose of this paper is to describe the general performance of the reanalysis data, detailed analyses of the year-to-year variations in the estimated emission sources will be discussed in a separate paper (Miyazaki et al., in preparation). This is noted in the manuscript.

References:

· Castellanos, P., and K. F. Boersma (2012), Reductions in nitrogen oxides over Europe driven by environmental policy and economic recession, Sci. Rep., 2, 265, doi:10.1038/srep00265.

· Gu, D., Y. Wang, C. Smeltzer, and Z. Liu (2013), Reduction in NOx emission trends over China: Regional and seasonal variations, Environ. Sci. Technol., 47(22), 12,912–12,919.

· Daniel Q. Tong, Lok Lamsal, Li Pan, Charles Ding, Hyuncheol Kim, Pius Lee, Tianfeng Chai, Kenneth E. Pickering, Ivanka Stajner, Long-term NOx trends over large cities in the United States during the great recession: Comparison of satellite retrievals, ground observations, and emission inventories, Atmospheric Environment, Volume 107, April 2015, Pages 70-84, ISSN 1352-2310, http://dx.doi.org/10.1016/j.atmosenv.2015.01.035.

1335: But there is no improvement visible actually at the surface? Or is the scale of the plot just such that this improvement isn't visible? While I don't doubt that including emissions leads to changes in the mid-trop, it seems it should though at least make an equal or lager improvement directly at the surface.

There are also improvements near the surface. The sentence has been rewritten as:

'At the NH mid-latitudes the changes introduced by optimizing the emission factors improve the agreement with the ozonesonde observation from April to August below about 500 hPa (Fig. 17) associated with the pronounced O_3 production caused by NOx increases; the monthly mean positive bias below about 900 hPa is reduced by 10-15 % in the summer and the negative bias between 900-500 hPa is reduced by 30-50 % in spring and summer.'

The improvement is larger in the middle troposphere than in the lower troposphere. This is probably because of larger spatial variations in the lower tropospheric O3 concentration and the coarse resolution of the model (i.e., larger representative error).

1342 - 1348: Shouldn't they both lead to the same O3 trends, the one which matches the observations, just by different means?

Because the interannual variation in the emissions was poorly represented in the a priori emissions (e.g., the anthropogenic emissions for 2008 were used in the calculation for 2010), the ozone concentration trend between 2005 and 2010 is expected to be unrealistic in the case without emission source inversion. In addition, the decreased number of TES measurements after 2010 makes it difficult to produce the ozone trend, particularly in the case without emission source inversion. Therefore, we can expect different ozone trends between the two calculations.

Table 6: The caption should state what is shown (percent error? ppb?), and if the values are model minus observations or vice versa.

Corrected.

Section 7.4.1: All though I'm not quite sure what the numbers in Table 6 represent (see previous comment), it seems odd that in the NH the differences at 200 hPA (16.3 vs 13.2) would be larger than differences at the surface (0.1 vs - 2.3) for the test using different prior emissions. Why would the impact of changing the prior emissions be greatest in the upper trop? Perhaps the results of this test would be better served by showing a plot of the difference in the posterior emissions between the standard and HTAP-based reanalysis.

The different a priori surface emissions led to differences in the estimated LNOx sources locally (at model grid point scale) by up to 15% at the NH mid-latitudes (the annual global total LNOx source differed by only 2%), which might cause the ozone concentration difference in the upper troposphere especially in the summer. The following sentence has been added:
'The spatial distribution of the estimated LNOx sources is also somewhat influenced by the choice of a priori surface emissions in the NH mid-latitudes (not shown), which led to differences in the agreement with the ozonesonde observation in the upper troposphere at 200 hPa.'

Section 7.6: Why not just report the uncertainty reduction as measured by the posterior / prior error, rather than the ensemble spread?

As described in the manuscript, the ensemble spread is influenced by errors in the model input data, chemical or physical parameters, numerical scheme, as well as errors in the measurements assimilated,

while it also reflects the instability of the tropospheric chemical system. We thus believe that measuring the absolute value of the estimated analysis spread (rather than the posterior/prior error ratio) is meaningful for the evaluation of the analysis uncertainty. The $\chi 2$ test provides further evidence that the ensemble spread is reasonable.

Section 7.7: I found the first half of this section (1620 - 1639) quite speculative. It could be removed, given the paper is already quite long.

The chemical reanalysis is still a challenging matter. However, its usefulness may not be well understood by many readers. We thus believe that this section is important and worth keeping, although it adds to the paper's length.

Conclusions: While the overall results of this work are indeed impressive, I feel there were a few aspects which need to be made more transparent, such as the inability to improve surface NO2 concentration in polluted areas, or the strange trends in NOx and CO emissions in the US and Europe. A bit more balanced evaluation of all strengths and weaknesses would be good.

To describe the weakness of the present study, the following sentence has been added:
'For instance, the reanalysis still has large negative biases in NO_2 concentrations over the polluted regions, which may be associated with errors in for instance the model chemical equilibrium states, planetary boundary layer (PBL) mixing, and diurnal variations of chemical processes and emissions.'

The estimated emissions show negative trends over the US and Europe, which will be described in a separate paper (Miyazaki et al., in preparation). Please also see my reply above.

4: retrieval data → data
53: to develop → in developing
55: information, → information
56: the estimates → estimates
121:),by→)by
247: the analysis performed → performing the analysis •
throughout: number % → number%
578: no new paragraph
619: too large → excessive
1151: while → while it

Corrected.

Author comments in reply to the anonymous referee on "A tropospheric chemistry reanalysis for the years 2005–2012 based on an assimilation of OMI, MLS, TES and MOPITT satellite data" by K. Miyazaki et al.

We want to thank the referee for the helpful comments, compliments on the quality of the manuscript and positive recommendation for our paper to be published. We have revised the manuscript according to the comments, and hope that the revised version of the manuscript is now suitable for publication. Below are the referee comments in italics with our replies in normal font.

Reply to Referee #2

Page 8690, Line 24: suggest clarifying what is meant by "bottom-up" in line with the description of "top-down" in the following sentence.

The sentence has been rewritten as follows:
'Currently available bottom-up inventories of emissions, produced based on statistical data such as emission related activities and emissions factors, contain large uncertainties'

Page 8693, Line 20: clarify that the 2.8 degree resolution is for longitude and latitude?

The sentence has been rewritten as follows:
'...T42 horizontal resolution (2.8° for longitude and the T42 Gaussian grid for latitude)...'

Page 8696, Line 15: the context for this sentence isn't very clear - suggest linking better to the previous sentence and clarifying that the optimization will lead to the reduction in the initial bias in the a priori emissions.

The sentences have been rewritten as follows:
'The emission sources were optimised at every analysis step throughout the reanalysis period, which reduced the initial bias in the a priori emissions during the data assimilation cycle.'

Page 8696, Line 18: suggest changing to "The EnKF approach always has. . .".

Corrected.

Page 8697, Line 1: suggest changing to "One difference to the study of. . ." .

Corrected.

Page 8697, Line 15: I' m not sure this statement on the averaging kernel is strictly true. The averaging kernels give the sensitivity of the retrieved state to the true state and the a priori dependence is only removed when the innovation is calculated, i.e. as in equation (4) and not in equation (7) which is what this statement appears to allude to. Please clarify this in the text.

The sentence has been rewritten as follows:
'The averaging kernel A defines the vertical sensitivity profile of the satellite observation. Even though the retrieval $\mathbf{y}^{\mathbf{0}}$ and the model equivalent $\mathbf{y_i^b}$ both depend on the a-priori, the use of the kernel removes the dependence of the analysis or the relative model--retrieval comparison $(\mathbf{y_i^b}-\mathbf{y}^{\mathbf{0}})/\mathbf{y_i^b}$ on the retrieval a-priori profile (Eskes and Boersma, 2003; Migliorini, 2012).'

Page 8698, Line 4: suggest using "simulation" or "model simulation" rather than "calculation".

Replaced by 'data assimilation calculation'.

Page 8698, Line 5: the sentence beginning "Eight series of..." isn' t very clear in its meaning, please rewrite and clarify.

The sentences have been rewritten as follows:
'Eight series of one-year calculations from the 1 January of each year in 2005-2012 with a two-month spin-up starting from the 1 November of the previous year were conducted to produce the eight-year reanalysis data set,. Each one-year run was parallelized on 16 processors. '

Page 8699, Line 12: I think "onboard" can be replaced with "on".

Replaced.

Page 8706, Line 7: Model underestimates of CO is a fairly persistent issue for a number of different models and the low bias relative to MOPITT shown in Figure 2 would appear to be consistent with this. It may be useful for the reader to acknowledge how the CHASER global CO field generally performs with respect to other models, and if this could also contribute to the OmF statistics in this study. This is

commented on in Section 5.2.1 but could also be mentioned here.

The following sentence has been added to the paragraph:
'The underestimation of tropospheric CO by CHASER was found to be very similar to that in most of the other CTMs (Shindell et al., 2006).'

Page 8707, Line 20: I think that this statement on the TES information content is consistent with the literature showing that the TES O3 averaging kernels have distinct peak sensitivities in the lower and upper troposphere – it would be useful to the reader if this was acknowledged/cited here.

The sentences have been rewritten as follows:
'Jourdain et al. (2007) showed that the TES retrievals have 1-2 DOFs in the troposphere, with the largest DOFs for clear-sky scenes occurring at low latitudes where TES can distinguish between lower and upper tropospheric O_3. The obtained analysis increments correspond well to the OmF in the control run at the same altitude (figure not shown), confirming that the data assimilation effectively reduced the model errors through the analysis steps.'

Page 8709, Line 1: I think "measurement" here should be "retrieval" to indicate that it refers to the satellite data as the ozonesondes don't have low sensitivity in the lower troposphere.

Replaced by 'retrieval'.

Page 8710, Line 28: Is it possible to back up the statement that the improvement in O3 relative to MOZAIC at cruise altitude is due to the MLS assimilation. Have the authors performed any sensitivity tests which quantify the relative contributions of the different assimilated datasets to the analysis? While it is clear that the MLS data could bring about this improvement, a supporting statement could be useful for the reader.

The sentences have been rewritten as follows:
'A substantial improvement is observed at the aircraft-cruising altitude around the tropopause (between 300 and 200 hPa) at the NH high-latitudes; the mean positive bias is reduced from +8 % in the control run to +3 % in the reanalysis. By separately assimilating individual measurements through the Observing System Experiments (OSEs), we confirmed that the improvement is mainly attributed to the MLS assimilation (not shown). '

Page 8711, Line 8: "attributing" should be "attributed".

Corrected.

Figures 9 and 13: I found each panel to generally be too small and could be made bigger using common y-axis titles.

Corrected.

¥documentclass[acpd, online, hvmath]{copernicus}

¥begin{document}¥hack{¥sloppy}

%¥documentclass[acp]{copernicus}

%¥begin{document}

¥linenumbers
~~¥begin{document}¥hack{¥sloppy}~~

~~%¥documentclass[acp]{copernicus}~~

~~%¥begin{document}~~

~~¥linenumbers~~

¥title{A~tropospheric chemistry reanalysis for the years 2005--2012 based on an assimilation of OMI, MLS, TES and MOPITT satellite data}

¥Author[1]{K.}{Miyazaki}
¥Author[2]{H.~J.}{Eskes}
¥Author[3]{K.}{Sudo}

¥affil[1]{Japan Agency for Marine-Earth Science and Technology, Yokohama 236-0001, Japan}
¥affil[2]{Royal Netherlands Meteorological Institute (KNMI), Wilhelminalaan 10, 3732 GK,¥hack{¥newline} De Bilt, the Netherlands}
¥affil[3]{Graduate School of Environmental Studies, Nagoya University, Nagoya, Japan}

¥runningtitle{Tropospheric chemistry reanalysis}
¥runningauthor{K.~Miyazaki et~al.}

¥correspondence{K.~Miyazaki (kmiyazaki@jamstec.go.jp)}

¥received{19~February~2015}
¥accepted{13~March~2015}
¥published{}

¥firstpage{1}

¥maketitle

¥begin{abstract}
We present the results from an eight-year tropospheric chemistry reanalysis for the period 2005--2012 obtained by assimilating multiple ~~retrieval~~ data sets from the OMI, MLS, TES, and MOPITT satellite instruments. The reanalysis calculation was conducted using a~global chemical transport model and an ensemble Kalman filter technique that simultaneously optimises the chemical concentrations of various species and emissions of several precursors. The optimisation of both the concentration and the emission fields is an efficient method to correct the entire tropospheric profile and its year-to-year variations, and to adjust various tracers chemically linked to the species assimilated. Comparisons against independent aircraft, satellite, and ozonesonde observations demonstrate the quality of the analysed ¥chem{O_3}, ¥chem{NO_2}, and ¥chem{CO} concentrations on regional and global scales and for both seasonal and year-to-year variations from the lower troposphere to the lower stratosphere. The data assimilation statistics imply persistent reduction of model error and improved representation of emission variability, but also show that discontinuities in the availability of the measurements lead to a~degradation of the reanalysis. The decrease in the number of assimilated measurements increased the ozonesonde minus analysis difference after 2010 and caused spurious variations in the estimated emissions. The Northern/Southern Hemisphere ¥chem{OH} ratio was modified considerably due to the multiple species

assimilation and became closer to an observational estimate, which played an important role in propagating observational information among various chemical fields and affected the emission estimates. The consistent concentration and emission products provide unique information on year-to-year variations of the atmospheric environment.

¥end{abstract}

¥introduction

Long-term records of the tropospheric composition of gases such as ozone (¥chem{O_3}), carbon monoxide (¥chem{CO}), and nitrogen oxides (¥chem{NO_x}) are important for understanding the changes in tropospheric chemistry and human activity and consequences for the atmospheric environment and climate change (HTAP, 2010; IPCC, 2013). Satellite instruments provide observations of the global distributions of tropospheric composition. For example, measurements of tropospheric ¥chem{O_3} have been retrieved using the Tropospheric Emission Spectrometer (TES) since 2004 (Beer, 2006) and by the Infrared Atmospheric Sounding Interferometer (IASI) since 2007 (Coman et~al., 2012). Tropospheric ¥chem{NO_2} column concentrations have been retrieved by the Ozone Monitoring Instrument (OMI) since 2004 (Levelt et~al., 2006), Scanning Imaging Absorption Spectrometer for Atmospheric Cartography (SCIAMACHY) from 2002--2012 (Bovensmann et~al., 1999), Global Ozone Monitoring Experiment (GOME) from 1996--2003, and GOME-2 since 2007 (Callies et~al., 2000). The availability of satellite-derived measurements of various chemical species has prompted increasing interest ~~to develop~~in developing methods for combining these sources of satellite observational information~~,~~ for studies of long-term variations within the atmospheric environment and for improving ~~the~~ estimates of emissions sources (Inness et~al., 2013; Streets et~al., 2013).

Combining measurements of ¥chem{O_3}, ¥chem{CO} and ¥chem{NO_x} in the atmosphere puts constraints on the concentration of ¥chem{OH}, the

main radical responsible for the removal of pollution from the atmosphere and determining the lifetime of many chemicals (Levy, 1971; Logan et~al., 1981; Thompson, 1992). At the same time the combined use provides constraints on different sources of surface emissions and production of ¥chem{NO_x} by lightning (¥chem{LNO_x}) (e.g., Martin et~al., 2007; Miyazaki et~al., 2014). The information that may be obtained from a~combined use of multiple satellite datasets without involving a~model is limited, related to differing vertical sensitivity profiles, different overpass times, and mismatches in spatial and temporal coverage between the instruments, as well as missing information on the chemical regime and origin of the air masses.

Data assimilation is the technique for combining different observational data sets with a~model, by considering the characteristics of each measurement (e.g., Kalnay, 2003; Lahoz and Schneider, 2014). Advanced data assimilation schemes like the Kalman filter or the related 4D-Var technique use the information provided by satellite-derived measurements and propagates it, in time and space, from a~limited number of observed species to a~wide range of chemical components to provide global fields that are physically and chemically consistent and in agreement with the observations. Various studies have demonstrated the capability of data assimilation techniques regarding the analysis of chemical species in the troposphere and stratosphere.

Assimilation of satellite limb measurements for ¥chem{O_3} profiles and nadir measurements for ¥chem{O_3} columns have been used to study ¥chem{O_3} variations in the stratosphere and the upper troposphere (e.g., Stajner and Wargan, 2004; Jackson, 2007; Stajner et~al., 2008; Wargan et~al., 2010; Flemming et~al., 2011; Barre et~al., 2013; Emili et~al., 2014). Long-term integrated data sets of stratospheric ¥chem{O_3} have been produced by several studies by combining multiple satellite retrieval datasets (e.g., Kiesewetter et~al., 2010; Van der A~et~al., 2010). The assimilation of satellite observations has been

also applied to investigate global variations in the tropospheric composition of gases such as ¥chem{O_3} and ¥chem{CO} (e.g., Parrington et~al., 2009; Coman et~al., 2012; Miyazaki et~al., 2012b). For providing long-term integrated data of tropospheric composition, as a~pioneer study, Inness et~al.~(2013) performed an eight-year reanalysis of tropospheric chemistry for 2003--2010 using an advanced data assimilation system. They included atmospheric concentrations of ¥chem{O_3}, CO, ¥chem{NO_x}, and formaldehyde (¥chem{CH_2O}) as the forecast model variables in the integrated forecasting system with modules for atmospheric composition (C-IFS), and they demonstrated improved ¥chem{O_3} and ¥chem{CO} profiles for the free troposphere. They also highlighted biases remaining in the lower troposphere associated with fixed surface emissions, which are not adjusted in the 4D-Var assimilation scheme presented by Inness et~al.~(2013).

Currently available bottom-up inventories of emissions, produced based on statistical data such as emission related activities and emissions factors, contain large uncertainties, mainly because of inaccurate activity rates and emission factors for each category and poor representation of their seasonal and interannual variations (e.g., Jaegl¥'{e} et~al., 2005; Xiao et~al., 2010; Reuter et~al., 2014). Top-down inverse approaches using satellite retrievals have been applied to obtain optimised emissions of ¥chem{CO} (e.g. Kopacz et~al., 2010; Hooghiemstra et~al., 2011) and ¥chem{NO_x} (e.g. Lamsal et~al., 2010; Miyazaki et~al., 2012a; Mijling et~al., 2013)~~,~~ by minimising the differences between observed and simulated concentrations, as summarised by Streets et~al.~(2013). In addition to surface emissions, the improved representations of ¥chem{LNO_x} sources are important for a~realistic representation of ¥chem{O_3} formation and chemical processes in the upper troposphere (Schumann and Huntrieser, 2007; Miyazaki et~al., 2014).

The simultaneous adjustment of emissions and concentrations of various species is a~new development in tropospheric chemical reanalysis and

long-term emissions analysis. Miyazaki et~al.~(2012b) developed a~data assimilation system, called CHASER-DAS, for the simultaneous optimization of the atmospheric concentration of various trace gases, together with an optimization of the surface emissions of ¥chem{NO_x} and ¥chem{CO}, and the ¥chem{LNO_x} sources, while taking their complex chemical interactions into account, as represented by the CHASER chemistry-transport model. Within the simultaneous optimisation framework, the analysis adjustment of atmospheric concentrations of chemically related species has the potential to improve the emission inversion (Miyazaki and Eskes, 2013; Miyazaki et~al., 2014). This was compared with an emission inversion based on measurements from one species alone, where uncertainties in the model chemistry affect the quality of the emission source estimates. In addition, the improved estimates of emissions benefit the atmospheric concentration analysis through a~reduction in model forecast error. The simultaneous adjustment of the emissions and the concentrations is therefore a~powerful approach to optimize all aspects of the chemical system influencing tropospheric ¥chem{O_3} (Miyazaki et~al., 2012b).

In this study, we present a~tropospheric chemistry reanalysis data set for the eight-year period from 2005 to 2012 using CHASER-DAS. This reanalysis is produced with the CHASER-DAS system introduced in Miyazaki et~al.~(2012b). The system uses the ensemble Kalman filter (EnKF) assimilation technique and assimilates Microwave Limb Sounder (MLS), OMI, TES, and Measurement of Pollution in the Troposphere (MOPITT) retrieved observations. The chemical concentrations and emission sources are simultaneously optimised during the reanalysis, and are expected to provide useful information for various research topics related to the inter-annual variability of the atmospheric environment and short-term trends.

The remainder of this paper is structured as follows. Section~2 describes the observations used for the assimilation and validation. Section~3 introduces the data assimilation system and Sect.~4 evaluates the reanalysis performance based on analyses of data

assimilation statistics. Section~5 presents comparisons against independent observations. Section~6 describes the emission source estimation results. Section~7, which discusses possible errors in the reanalysis data and offers thoughts on future developments, is followed by the conclusions in Sect.~8.

¥section{Data assimilation system}

The CHASER-DAS system (Miyazaki et~al., 2012a, b, 2014; Miyazaki and Eskes, 2013) has been developed based on an EnKF approach and a~global chemical transport model called CHASER. The data assimilation settings used for the reanalysis calculation are mostly the same as in Miyazaki et~al.~(2014), but the calculation was extended to cover the eight years from 2005--2012, and several updates were applied to the a~priori and state vector settings. Brief descriptions of the forecast model, data assimilation approach, and experimental settings are presented below.

¥subsection{Forecast model}

The CHASER model (Sudo et~al., 2002, 2007) was used as a~forecast model. It has so-called T42 horizontal resolution (2.8{¥degree} for longitude and the T42 Gaussian grid for latitude) and
32 vertical levels from the surface to 4¥,¥unit{hPa}. It is coupled to the atmospheric general circulation model (AGCM) version 5.7b of the Center for Climate System Research and Japanese National Institute for Environmental Studies (CCSR/NIES). Meteorological fields are provided by the AGCM at every time step of CHASER (i.e., every 20¥,¥unit{min}). The AGCM fields were nudged toward the National Centers for Environmental Prediction/Department of Energy Atmospheric Model Intercomparison Project II (NCEP-DOE/AMIP-II) reanalysis (Kanamitsu et~al., 2002) at every time step of the AGCM to reproduce past meteorological fields. The nudged AGCM enabled us to perform CHASER calculations that included short-term atmospheric variations and parameterised transport processes by sub-grid-scale convection and

boundary layer mixing.

The a~priori value for surface emissions of ¥chem{NO_x} and ¥chem{CO} were obtained from bottom-up emission inventories. Anthropogenic ¥chem{NO_x} and ¥chem{CO} emissions were obtained from the Emission Database for Global Atmospheric Research (EDGAR) version 4.2. Emissions from biomass burning are based on the monthly Global Fire Emissions Database (GFED) version 3.1 (van der Werf et~al., 2010). Emissions from soils are based on monthly mean Global Emissions Inventory Activity (GEIA) (Graedel et~al., 1993). EDGAR version 4.2 was not available after 2008 at the time the reanalysis was started; therefore, the emissions for 2008 were used in the calculations for 2009--2012. GFED 3.1 was not available for 2012 and thus, the emissions averaged over 2005--2011 were used in the calculation for 2012. For surface ¥chem{NO_x} emissions, a~diurnal variability scheme developed by Miyazaki et~al.~(2012) was applied depending on the dominant category for each area: anthropogenic, biogenic, and soil emissions.

For the calculation of a~priori ¥chem{LNO_x} emissions, the global distribution of the flash rate was parameterised in CHASER for convective clouds based on the relation between lightning activity and cloud top height (Price and Rind, 1992). To obtain a~realistic estimate of the global annual total flash occurrence, a~tuning factor was applied for the global total frequency, which is independent of the lightning adjustment in the assimilation. The global distribution of the total flash rate is generally reproduced well by the model in comparison with the observations, except for overestimations over northern South America and underestimations over both Central Africa and most of the oceanic intertropical convergence zone (Miyazaki et~al., 2014).

¥subsection{Data assimilation technique}

The data assimilation technique employed is an EnKF approach, i.e.,

a~local ensemble transform Kalman filter (LETKF, Hunt et~al., 2007) based on the ensemble square root filter (SRF) method, which uses an ensemble forecast to estimate the background error covariance matrix. The covariance matrices of the observation error and background error determine the relative weights given to the observation and the background in the analysis. ~~The advantage of the EnKF over 4D-VAR is its simple implementation for complicated systems such as CTMs.~~ The LETKF has conceptual and computational advantages over the original EnKF. First, the analysis is performed locally in space and time, which reduces sampling errors caused by limited ensemble size. Second, performing ~~the analyses~~ analysis ~~performed~~ independently for different grid points allow parallel computations to be performed that reduce the computational cost. These advantages are important in the chemical reanalysis calculation because of the many analysis steps included in the eight-year reanalysis run and the large state vector size used for the multiple states optimisation (cf., Sects.~2.3 and 2.7).

The assimilation step transforms a background ensemble ($¥vec{x}_{i}^¥mathrm{b}; i=1,¥ldots, k$) into an analysis ensemble ($¥vec{x}_{i}^¥mathrm{a}; i=1,¥ldots, k$) and updates the analysis mean, where ¥vec{x} represents the model variable, $¥mathrm{b}$ the background state, $¥mathrm{a}$ the analysis state, and k the ensemble size. The forecast and analysis steps are described briefly below.

¥subsubsection{The forecast step}

In the forecast step, the ~~The~~ background ensemble mean $¥overline{¥vec{x}^{¥mathrm{b}}}$ and its perturbation $¥mathbf{X}^{¥mathrm{b}}$ are obtained from the evolution of each ensemble member using the forecast model at every model grid,

¥begin{align}
 &
¥overline{¥vec{x}^{¥mathrm{b}}}=¥frac{1}{k} ¥sum^{k}_{i=1} ¥vec{x}_{i}^{¥mathrm{b}};

¥quad ¥mathbf{X}_{i}^{¥mathrm{b}}=¥vec{x}_{i}^{¥mathrm{b}}-¥overline{¥vec{x}^{¥mathrm{b}}}.

¥end{align}

$¥mathbf{X}^¥mathrm{b}_{i}$ is the ith column of an ~~$¥mathbf{X}^{¥mathrm{b}}$ is an~~ $N ¥times k$ matrix $¥mathbf{X}^{¥mathrm{b}}$, where N indicates the system dimension (the state vector size times the physical system dimension) ~~and k represents the ensemble size~~. Based on the assumption that background ensemble perturbations $¥mathbf{X}^{¥mathrm{b}}$ sample the forecast errors, the background error covariance is estimated as follows:

¥begin{align}

&

¥mathbf{P}^{¥mathrm{b}}=¥mathbf{X}^{¥mathrm{b}}(¥mathbf{X}^{¥mathrm{b}})^T,

¥end{align}

where the background error covariance $¥mathbf{P}^{¥mathrm{b}}$ varies with time and space, reflecting dominant atmospheric processes and locations of the observations.

An ensemble of background vectors $¥vec{y}_i^{¥mathrm{b}}$ and an ensemble of background perturbations in the observation space $¥mathbf{Y}^{¥mathrm{b}}$ are estimated using the observation operator H (cf., Sect.~2.5):

¥begin{align}

&

¥vec{y}_i^{¥mathrm{b}} =H ¥left(¥vec{x}_{i}^{¥mathrm{b}}¥right); ¥mathbf{Y}_i^{¥mathrm{b}}=¥vec{y}^{¥mathrm{b}}_i-¥overline{¥vec{y}^{¥mathrm{b}}}.

¥end{align}

¥subsubsection{The analysis step}

The analysis ensemble mean is obtained by updating the background ensemble mean:

¥begin{align}

&

¥overline{¥vec{x}^{{a}}}=¥overline{¥vec{x}^{¥mathrm{b}}}+ ¥mathbf{X}^{¥mathrm{b}} ¥tilde{¥mathbf{P}}^{{a}} (¥mathbf{Y}^{¥mathrm{b}})^T ¥mathbf{R}^{-1} (¥vec{y}^{¥mathrm{o}} - ¥overline{¥vec{y}^{¥mathrm{b}}}),

¥end{align}
where $¥vec{y}^{¥mathrm{o}}$ represents the observation vector, $¥mathbf{R}$ is the $p ¥times p$ observation error covariance, and p indicates the number of observations. The observation error information is obtained for each retrieval (cf., Sect.~2.6), where $¥tilde{¥mathbf{P}}^{¥mathrm{a}}$ is the $k ¥times k$ local analysis error covariance in the ensemble space:

¥begin{align}
 &
¥tilde{¥mathbf{P}}^{¥mathrm{a}} =
¥left[¥frac{(k-1) I}{1+¥Delta} + ¥big(¥mathbf{Y}^{¥mathrm{b}}¥big)^{¥mathrm{T}} ¥mathbf{R}^{-1} ¥mathbf{Y}^{¥mathrm{b}} ¥right]^{-1}.
¥end{align}

A~covariance inflation factor ($¥Delta=6$¥,{¥%}) was applied to inflate the forecast error covariance at each analysis step. The inflation is used to prevent an underestimation of background error covariance and resultant filter divergence caused by model errors and sampling errors. The estimation of the $¥tilde{¥mathbf{P}}^{¥mathrm{a}}$ matrix does not require any calculation of large vectors or matrices with N dimensions in the LETKF algorithm.

The new analysis ensemble perturbation matrix in the model space ($¥mathbf{X}^{¥mathrm{a}}$) is obtained by transforming the background ensemble $¥mathbf{X}^{¥mathrm{b}}$ with $¥tilde{¥mathbf{P}}^{¥mathrm{a}}$:

¥begin{align}
 &
¥mathbf{X}^{¥mathrm{a}} =
¥mathbf{X}^{¥mathrm{b}} ¥left[(k-1) ¥tilde{¥mathbf{P}}^{¥mathrm{a}} ¥right]^{1/2}.
¥end{align}

The new ensemble members ~~background error covariance~~ $¥vec{x}_{i}^{¥mathrm{b}}$ ~~for~~ after the next forecast step ~~is~~are then obtained from ~~a~~model simulations starting from the analysis ensemble $¥vec{x}_{i}^{¥mathrm{a}}$.

¥subsection{State vector}

The state vector for the reanalysis calculation is chosen to optimise the tropospheric chemical system and to improve the reanalysis performance. The state vector used in the reanalysis includes several emission sources (surface emissions of ¥chem{NO_x} and ¥chem{CO}, and ¥chem{LNO_x} sources) as well as the predicted concentrations of 35 chemical species~~,~~. The chemical concentrations in the state vector are expressed in the form of volume mixing ratio, while the emissions are represented by ~~in the form of a~~ scaling factors ~~–~~for each surface grid cell for the ~~complete~~ total ¥chem{NO_x} and ¥chem{CO} emissions at the surface (not for individual sectors), and for each production rate profile of the ¥chem{LNO_x} sources. Perturbations obtained by adding these model parameters into the state vector introduced an ensemble spread of chemical concentrations and emissions in the forecast step. The background error correlations, estimated from the ensemble model simulations at each analysis step, determine the relationship between the concentrations and emissions of related species, which can reflect daily, seasonal, interannual, and geographical variations in transport and chemical reactions. The emission sources were optimised at every analysis step throughout the reanalysis period, which reduced ~~. T~~the initial bias in the a~priori emissions ~~can be reduced gradually through~~ during the data assimilation cycle.

¥subsection{Covariance localisation}

The EnKF approach~~es~~ always ~~have~~ has the problem of introducing unrealistic long distance error correlations because of the limited number of ensemble members. During the reanalysis calculation, such spurious correlations lead to errors in the fields that may accumulate and will influence the reanalysis quality in a~negative way. In order to improve the filter performance, the covariance among non- or weakly related variables in the state vector is set to zero based on sensitivity calculation results, as in Miyazaki et~al.~(2012b). The

analysis of surface emissions of ¥chem{NO_x} and ¥chem{CO} allowed for error correlations with OMI ¥chem{NO_2} and MOPITT ¥chem{CO} data, while those with other data were neglected. For the ¥chem{LNO_x} sources, covariances with MOPITT ¥chem{CO} data were neglected. Concentrations of ¥chem{NO_y} species and ¥chem{O_3} were optimised from TES ¥chem{O_3}, OMI ¥chem{NO_2}, and MLS ¥chem{O_3} and ¥chem{HNO_3} observations. One difference to the study of ~~Different from the study of~~ Miyazaki et~al.~(2012b) is that~~,~~ concentrations of non-methane hydrocarbons (NMHC) were not optimised in the reanalysis. The assimilation of MOPITT ¥chem{CO} data led to concentrations of NMHC that increased to unrealistic values during the reanalysis, likely associated with too much chemical destruction of ¥chem{CO} (cf., Sect.~7.4.2).

Covariance localization was also applied to avoid the influence of remote observations, which is described in Sect.~2.7.

¥subsection{Observation operator}

The observation operator (H) includes the spatial interpolation operator (S), a~priori profile ($¥vec{x}_{¥text{apriori}}$), and averaging kernel ($¥vec{A}$), which maps the model fields ($¥vec{x}_{i}^{¥mathrm{b}}$~~¥vec{x}^{¥mathrm{b}}~~$) into retrieval space ($¥vec{y}_i^{¥mathrm{b}}$) thereby accounting for the vertical averaging implicit in the observations, as follows:

¥begin{align}
&
¥vec{y}_i^{¥mathrm{b}}~~¥vec{y}^{¥mathrm{b}}~~= H(¥vec{x}_{i}^{¥mathrm{b}}~~¥vec{x}^{¥mathrm{b}}~~) = ¥vec{x}_{¥text{apriori}} + ¥vec{A}(S(¥vec{x}_i^{¥mathrm{b}})-¥vec{x}_{¥text{apriori}}),
¥end{align}

where $¥vec{x}_i^{¥mathrm{b}}$ is the N-dimensional state vector and $¥vec{y}_i^{¥mathrm{b}}~~¥vec{y^{¥mathrm{b}}}~~$ is the p-dimensional model equivalent of the

observational vector. The averaging kernel $¥vec{A}$ defines the vertical sensitivity profile of the satellite observation. Even though the retrieval $¥vec{y}^{¥mathrm{o}}$ and the model equivalent $¥vec{y}_i^{¥mathrm{b}}$ both depend on the a-priori, the use of the kernel removes the dependence of the analysis or the relative model--retrieval comparison ($¥vec{y}_i^{¥mathrm{b}}-¥vec{y}^{¥mathrm{o}}$)/$¥vec{y}_i^{¥mathrm{b}}$ on the retrieval a-priori profile (Eskes and Boersma, 2003; Migliorini, 2012).~~The averaging kernel ($¥vec{A}$) defines the vertical sensitivity profile of the satellite retrievals and removes the dependence of the analysis on the retrieval a-priori profile (Eskes and Boersma, 2003).~~

¥subsection{Observation error}

The observation error provided in the retrieval data products includes contributions from the smoothing errors, model parameter errors, forward model errors, geophysical noise, and instrument errors. In addition, a~representativeness error was added for the OMI ¥chem{NO_2} and MOPITT ¥chem{CO} observations to account for the spatial resolution differences between the model and the observation using a~super-observation approach following Miyazaki et~al.~(2012a). The super-observation error was estimated by considering an error correlation of 15¥,{¥%} among the individual satellite observations within a~model grid cell.

¥subsection{Reanalysis settings}

Because a~single continuous data assimilation calculation for eight years requires a~long computational time, we parallelised the reanalysis calculation. Eight series of one-year calculations from the 1 January of each year in 2005--2012~~were conducted for 2005–2012,~~ with a~two-month spin-up starting from the 1 November of the previous year were conducted to produce the eight-year reanalysis data set.~~, whereas e~~ Each one-year run was parallelized on 16 processors. The two-month spin-up removed the differences in the analysis between the different time series, providing a~continuous

eight-year data set. Because of distinct diurnal variations in the tropospheric chemical system, the data assimilation cycle was set to be short (i.e., 120¥,¥unit{min}) to reduce sampling errors. The emission and concentration fields were analysed and updated at every analysis step.

In the reanalysis calculation the ensemble size was set to 30, which is somewhat smaller than the 48 members used in our previous studies. A~smaller ensemble size reduces computational cost, but slightly degrades analysis performance, as quantified in Miyazaki et~al.~(2012b). The horizontal localisation scale L was set to 450¥,¥unit{km} for ¥chem{NO_x} emissions and to 600¥,¥unit{km} for ¥chem{CO} emissions, ¥chem{LNO_x}, and for the concentrations. The physical vertical localization length was set to ln(P1/P2) [hPa] = 0.2. These choices are based on sensitivity experiments (Miyazaki et~al., 2012b), for which the influence of an observation was set to zero when the horizontal distance between the observation and analysis point was larger than $2L¥times¥sqrt{10/3}$ (the cut off radius is set to 2191 ¥unit{km} for L = 600 ¥unit{km}). We also account for the influence of the averaging kernels of the instruments, which captures the vertical sensitivity profiles of the retrievals. The ensemble members and ensemble spread (error covariance) do vary from one location to the next, and from one species to the next, thereby representing the large number of degrees of freedom contained in the model and they way these are constrained by the observations.~~.~~

The a~priori error was set to 40¥,{¥%} for surface emissions of ¥chem{NO_x} and ¥chem{CO} and 60¥,{¥%} for ¥chem{LNO_x} sources, but a~model error term was not implemented for emissions during the forecast. To prevent covariance underestimation and maintain emission variability during the long-term reanalysis calculation, we applied covariance inflation to the emission source factors in the analysis step, i.e., model error is implemented through a~covariance inflation term. The standard deviation was artificially inflated to a~minimum predefined value (30¥,{¥%} of the initial standard deviation) at each analysis step. This was found to be important for representing

realistic seasonal and interannual variability in the emission estimates, as confirmed by the improved agreements between the predicted concentrations and independent observations when this emission covariance inflation setting is used.

In addition to the standard reanalysis run, we conducted a~control run for the eight-year period from 2005 to 2012 and several sensitivity calculations for 2005 and 2010 by changing the data assimilation settings. The control run was performed without any data assimilation, but using the same model settings as used in the reanalysis run. The settings and results of sensitivity calculations are presented in Sect.~7.

¥section{Observations}

¥subsection{Assimilated data sets}

The assimilated observations were obtained from the OMI, TES, and MLS ~~onboard~~ on the Aura satellite, launched in July~2004 and from MOPITT on~~board~~ Earth Observing System (EOS) Terra, which was launched in December~1999.

¥subsubsection{OMI tropospheric ¥chem{NO_2} column}

The OMI provides measurements of both direct and atmosphere-backscattered sunlight in the ultraviolet--visible range (Levelt et~al., 2006). The reanalysis used tropospheric ¥chem{NO_2} column retrievals obtained from the version-2 DOMINO data product (Boersma et~al., 2011). The analysis increments in the assimilation of OMI ¥chem{NO_2} were limited to adjust only the surface emissions of ¥chem{NO_x}, ¥chem{LNO_x} sources, and concentrations of ¥chem{NO_y} species. Low-quality data were excluded before assimilation following the recommendations of the product's specification document (Boersma et~al., 2011). Since December~2009, approximately half of the pixels have been compromised by the so-called row anomaly which reduced the

daily coverage of the instrument.

¥subsubsection{TES ¥chem{O_3}}

The TES ¥chem{O_3} data used are the version 5 level 2 nadir data obtained from the global survey mode (Herman and Kulawik, 2013). This data set consists of 16 daily orbits with spatial resolution of 5--8¥,¥unit{km} along the orbit track. The vertical resolution of TES ¥chem{O_3} profile retrievals is typically 6¥,¥unit{km} in the tropics and in the summer hemisphere for cloud free conditions (Worden et~al., 2004). The standard quality flags were used to exclude low-quality data (Herman and Kulawik, 2013). We also excluded data poleward of 72{¥degree}, because of the small retrieval sensitivity. The data assimilation was performed based on the logarithm of the mixing ratio following the retrieval product specification.

¥subsubsection{MLS ¥chem{O_3} and ¥chem{HNO_3}}

The MLS data used are the version 3.3 ¥chem{O_3} and ¥chem{HNO_3} level 2 products (Livesey et~al., 2011). We excluded tropical-cloud-induced outliers, following the recommendations in Livesey et~al.~(2011). We used data for pressures lower than 215¥,¥unit{hPa} for ¥chem{O_3} and 150¥,¥unit{hPa} for ¥chem{HNO_3} to constrain the ¥chem{LNO_x} sources and concentration of ¥chem{O_3} and ¥chem{NO_y} species. The accuracy and precision of the measurement error, described in Livesey et~al.~(2011), were included as the diagonal element of the observation error covariance matrix.

¥subsubsection{MOPITT CO}

The MOPITT ¥chem{CO} data used are the version 6 level 2 TIR products (Deeter et~al., 2013). The MOPITT instrument is mainly sensitive to free tropospheric ¥chem{CO}, especially in the middle troposphere, with Degrees of Freedom for signal (DOFs) typically much larger than 0.5. We excluded data poleward of

65{¥degree} and during nighttime because of data quality problems (Heald et~al., 2004). The data at 700¥,¥unit{hPa} were used for constraining the surface ¥chem{CO} emissions.

¥subsection{Validation data sets}

For the comparisons with satellite observations, the model concentrations were interpolated to the retrieval pixels at the overpass time of the satellite while applying the averaging kernel of each retrieval, and then both the retrieved and simulated concentrations are mapped on a~horizontal grid with a~resolution of 2.5{¥degree}¥,$¥times$¥,2.5{¥degree}. For comparisons with aircraft and ozonesonde observations, the data were binned on a~pressure grid with an interval of 30¥,¥unit{hPa} and mapped with a~horizontal resolution of 5.0{¥degree}¥,$¥times$¥,5.0{¥degree}, while the model output was interpolated to the time and space of each sample.

¥subsubsection{GOME-2 and SCIAMACHY ¥chem{NO_2}}

Tropospheric ¥chem{NO_2} retrievals were obtained from the TEMIS website (¥url{www.temis.nl}) and consists of the version 2.3 GOME-2 and SCIAMACHY products (Boersma et~al., 2011). The ground pixel size of the GOME-2 retrievals is 80¥,¥unit{km}¥,$¥times$¥,40¥,¥unit{km} with a~global coverage within 1.5 days, whereas that of the SCIAMACHY retrievals is 60¥,¥unit{km}¥,$¥times$¥,30¥,¥unit{km} with global coverage provided approximately once every six days. The equatorial overpass times of GOME-2 and SCIAMACHY are at 09:30 and 10:00¥,LT, respectively. Observations with radiance reflectance of < 50¥,{¥%} from clouds with quality flag = 0 were used for validation.

¥subsubsection{MOZAIC/IAGOS aircraft data}

Aircraft ¥chem{O_3} and ¥chem{CO} measurements obtained from the Measurement of Ozone, Water Vapor, Carbon Monoxide, Nitrogen Oxide by Airbus In-Service Aircraft/In service Aircraft for Global Observing

System (MOZAIC/IAGOS) programmes (Petzold et~al., 2012; Zbinden et~al.,~2013) were used to validate the tropospheric profiles near airports and the upper tropospheric spatial distributions at flight altitude of about 12¥,¥unit{km} in the NH and some parts of the tropics. The data are available at ¥url{www.iagos.fr}. The measurements of ¥chem{O_3} and ¥chem{CO} have an estimated accuracy of $¥pm$(2¥,¥unit{ppb}¥,$+$¥,2¥,{¥%}) and $¥pm$5¥,¥unit{ppb} ($¥pm$5¥,{¥%}), respectively (Zbinden et~al.,~2013).

¥subsubsection{HIPPO aircraft data}

HIAPER Pole-to-Pole Observation (HIPPO) aircraft measurements provide global information on vertical profiles of various species over the Pacific (Wofsy et~al.,~2012). Latitudinal and vertical variations of ¥chem{O_3} and ¥chem{CO} obtained from the five HIPPO campaigns (HIPPO I, 8--30 January~2009; HIPPO II, 31 October to 22 November~2009; HIPPO III, 24 March to 16 April~2010; HIPPO IV, 14 June to 11 July~2011; and HIPPO V, 9 August to 9 September~2011) were used to validate the assimilated profiles.

¥subsubsection{NASA Aircraft campaign data}

Vertical profiles of seven key gases (¥chem{O_3}, ¥chem{CO}, ¥chem{NO_2}, ¥chem{OH}, ¥chem{HO_2}, ¥chem{HNO_3}, and ¥chem{CH_2O}) obtained from six aircraft campaigns: Intercontinental Chemical Transport Experiment -- Phase B (INTEX-B), Arctic Research of the Composition of the Troposphere from Aircraft and Satellites (ARCTAS)-A, ARCTAS-B, Deriving Information on Surface Conditions from Column and Vertically Resolved Observations Relevant to Air Quality (DISCOVER-AQ), Deep Convection Clouds {¥&} Chemistry (DC3)-DC8, and DC3-GV were used.

The DC-8 measurements obtained during the INTEX-B campaign over the Gulf of Mexico (Singh et~al., 2009) were used for the comparison for March~2006. Data collected over highly polluted areas (over Mexico City and Houston) were removed from the comparison, because they can

cause serious errors in representativeness (Hains et~al., 2010).

The NASA Arctic Research of the Composition of the Troposphere from Aircraft and Satellites (ARCTAS) mission (Jacob et~al., 2010) was conducted in two three-week deployments based in Alaska (April~2008, ARCTAS-A) and western Canada (June--July~2008, ARCTAS-B). During ARCTAS-A, most of the measurements were collected between 60--90{¥degree}¥,N, whereas during ARCTAS-B, the measurements were mainly recorded in the sub-Arctic between 50--70{¥degree}¥,N.

During the NASA DISCOVER-AQ campaign over Baltimore (US) in July~2011, the NASA P-3B aircraft performed extensive profiling of the optical, chemical, and microphysical properties of aerosols (Crumeyrolle et~al., 2014).

The Deep Convective Clouds and Chemistry Project (DC3) field campaign investigated the impact of deep, mid-latitude continental convective clouds, including their dynamical, physical, and lightning processes, on upper tropospheric composition and chemistry during May and June~2012 (Barth et~al., 2015). The observations were conducted in three locations, northeastern Colorado, west Texas to central Oklahoma, and northern Alabama. The observations obtained from the DC-8 (DC3-DC8) and G-V (DC3-GV) aircrafts were used.

¥subsubsection{Ozonesonde data}

Ozonesonde observations taken from the World Ozone and Ultraviolet radiation Data Center (WOUDC) database (available at ¥url{http://www.woudc.org}) were used to validate the vertical ¥chem{O_3} profiles. All available data from the WOUDC database are used for the validation (totally 19¥,273 profiles for 149 stations during 2005--2012). The observation error is 5--10¥,{¥%} between 0--30¥,¥unit{km} (Smit et~al., 2007).

¥subsubsection{WDCGG ¥chem{CO}}

The ¥chem{CO} concentration observations were obtained from the World Data Centre for Greenhouse Gases (WDCGG) operated by the World Meteorological Organization (WMO) Global Atmospheric Watch program (¥url{http://ds.data.jma.go.jp/gmd/wdcgg/}). Hourly and event observations from 59 stations were used to validate the surface ¥chem{CO} concentrations.

¥section{Data assimilation statistics}

¥subsection{$¥chi^2$ diagnosis}

The long-term stability of the data assimilation performance is important in evaluating the reanalysis. The $¥chi^2$ test can be used to evaluate the data assimilation balance (e.g. M¥'{e}nard and Chang, 2000), which is estimated from the ratio of the actual Observation-minus-Forecast (OmF: $¥vec{y}^{¥mathrm{o}} - H ¥left(¥vec{x}^{¥mathrm{b}} ¥right)$) to the sum of the estimated model and observation error covariances in the observational space ($¥mathbf{H} ¥mathbf{P}^{¥mathrm{b}} ¥mathbf{H}^T + ¥mathbf{R}$), as follows:

¥begin{align}
  &
¥mathbf{Y} = ¥frac{1} {¥sqrt{m}}
(¥mathbf{H} ¥mathbf{P}^{¥mathrm{b}} ¥mathbf{H}^T + ¥mathbf{R}) ^{-1/2}
(¥vec{y}^{¥mathrm{o}} - H ¥left(¥vec{x}^{¥mathrm{b}} ¥right)),
¥¥
  &
¥chi^2 = ¥text{trace} ¥mathbf{Y}¥mathbf{Y}^T,
¥end{align}

where m is the number of observations. $¥chi^2$ becomes 1 if the background error covariances ($¥mathbf{P}^{¥mathrm{b}}$) are properly determined to match with the observed OmF ($¥vec{y}^{¥mathrm{o}} - H ¥left(¥vec{x}^{¥mathrm{b}} ¥right)$) under the presence of the

prescribed observation error ($¥mathbf{R}$).

Figure~1 shows the temporal evolution of the number of assimilated observations (m) and $¥chi^2$ for each assimilated measurement type. The number of super observation is shown for the OMI ¥chem{NO_2} and MOPITT ¥chem{CO}. For most cases, the mean values of $¥chi^2$ are generally within 50¥,{¥%} difference from the ideal value of 1, which suggests that the forecast error covariance is reasonably well specified in the data assimilation throughout the reanalysis. Note that the covariance inflation factor for the concentrations and emissions were optimized to approach to the ideal value based on sensitivity experiments (Miyazaki et~al., 2012b). For the OMI ¥chem{NO_2} assimilation, the $¥chi^2$ is > 1, which indicates overconfidence in the model or underestimation of the super-observation error (computed as a combination of the measurement error and the representativeness error). The $¥chi^2$ for the OMI ¥chem{NO_2} was less sensitive to the choice of the inflation factor compared to that for other assimilated measurements. Lower tropospheric ¥chem{NO_2} is controlled by fast chemical reactions restricted by biased chemical equilibrium states, leading to an underestimation of the background error covariance during the forecast. Although the emission analysis introduces spread to the concentration ensemble, the perturbations are present primarily near the surface and tend to be removed in the free troposphere because of the short chemical lifetime of ¥chem{NO_x}.

~~Overall~~Before 2010, the annual mean $¥chi^2$ is roughly constant ~~throughout the reanalysis~~, which confirms the good stability of the performance. ~~However, s~~Seasonal and interannual~~–~~ variations, especially after 2010, of ~~the~~ $¥chi^2$ can be attributed to variations in the coverage and quality of satellite retrievals as well as changes in atmospheric conditions (e.g., chemical lifetime and dominant transport type). The increased $¥chi^2$ for OMI ¥chem{NO_2} after 2010 is associated with a~decrease in the number of the assimilated measurements and changes in the super observation error. Both the mean measurement error and the representativeness error (a~function of the number of OMI observations) are typically larger in 2010--2012 than in

2005--2009; the mean measurement error and the total super observation error (a~sum of the measurement error and the representativeness error) averaged over 30--55{¥degree}¥,N in January are about 7 and 9¥,{¥%} larger in 2010--2012 than in 2005--2009, respectively. After 2010, the ~~too large~~excessive $¥chi^2$ indicates underestimations in the analysis spread, while the increased OmF indicates smaller corrections by the assimilation (cf., Sect.~4.2). To correct the concentrations and emission from OMI super observations that have larger super observation errors, the forecast error needs to be further inflated. A~technique to adaptively inflate the forecast error covariance for the concentrations and emissions of ¥chem{NO} and ¥chem{NO_2} is required to better represent the data assimilation balance throughout the reanalysis.

¥subsection{OmF}

OmF statistics are computed in observation space to investigate the structure of model--observation differences and to measure improvements in the reanalysis (Fig.~2). Model biases, as measured from the OmF in the control run, are persistent throughout the reanalysis period and vary considerably with season. The figure shows an underestimation (i.e., positive OmF) of tropospheric ¥chem{NO_2} columns compared with the OMI ¥chem{NO_2} data from the SH subtropics to NH mid-latitudes, an underestimation of tropospheric ¥chem{CO} compared with MOPITT ¥chem{CO} data in the NH, an overestimation (i.e., negative OmF) of middle and upper tropospheric ¥chem{O_3} in the extratropics compared with TES and MLS ¥chem{O_3} data, and underestimation of middle tropospheric ¥chem{O_3} in the tropics compared with TES. The underestimation of tropospheric ¥chem{CO} by CHASER was found to be very similar to that in most of the other CTMs (Shindell et al., 2006).

After 2010, the positive OmF for MOPITT ¥chem{CO} in the control run decreases in the NH, and the positive OmF for OMI ¥chem{NO_2} increases in the NH mid-latitudes. As the quality of these retrievals is considered constant in the reanalysis period (e.g., Worden et~al.,

2013), the interannual variations of OmF are probably attributed to long-term changes in the model bias. The anthropogenic emission inventories for 2008 were used in the model simulation for 2009--2012, which could be partly responsible for the absence of a~concentration trend in the model._

In the reanalysis run, the OmF bias and RMSE for MLS ¥chem{O_3} becomes nearly zero globally because of the assimilation. The systematic reductions of the OmF confirm the continuous corrections for model errors by the assimilation. The remaining error is almost equal to the mean observational error. The OmF reduction is relatively smaller for MLS ¥chem{HNO_3} than for MLS ¥chem{O_3} because of the larger observational errors.

The mean OmF bias against TES ¥chem{O_3} data in the middle troposphere is almost completely removed because of the assimilation, and the mean OmF RMSE is reduced by about 40¥,{¥%} in the SH extratropics and by up to 15¥,{¥%} from the tropics to the NH. The error reduction is weaker in the lower troposphere (figure not shown) because of the reduced sensitivity of the TES retrievals to lower tropospheric ¥chem{O_3}. The analysed OmF becomes larger after 2010 corresponding to the decreased number of assimilated measurements.

Data assimilation removes most of the OmF bias against MOPITT ¥chem{CO} data with a~mean bias (RMSE) reduction of about 85¥,{¥%} (60¥,{¥%}) in the NH extratropics and about 80¥,{¥%} (30¥,{¥%}) in the tropics, respectively. The annual mean OmF becomes almost constant through the reanalysis, suggesting that the a~posteriori emissions realistically represent the interannual variations.

The mean OmF bias against OMI ¥chem{NO_2} is reduced with a~mean reduction of about 30--60¥,{¥%} at the NH mid-latitudes and about 50--60¥,{¥%} in the tropics. The remaining errors could be associated with the short chemical lifetime of ¥chem{NO_x} in the boundary layer

as compared to the OMI revisit time of roughly one day, biases in the simulated chemical equilibrium state, and the underestimation of the emission spread. The OmF is relatively larger in 2010--2012 than in other years, corresponding to about half the reduction in the OMI ¥chem{NO_2} observation. The number of assimilated measurements is important for reducing model errors, even when global coverage is provided. The mean Observation-minus-Analysis (OmA) bias is about 10--15¥,{¥%}; it is smaller in the NH mid-latitudes and almost the same in the tropics and SH compared with the mean OmF in the reanalysis (figure not shown).

¥subsection{Analysis increment}

The analysis increment information, estimated from the differences between the forecast and the analysis both in the reanalysis run, is a~measure of the adjustment made in the analysis step. The analysis increment for ¥chem{O_3} is mostly positive at 700¥,¥unit{hPa} and negative at 400¥,¥unit{hPa} at mid latitudes (Fig.~3). The positive (negative) increments imply that the short-term model forecast underestimates (overestimates) the ¥chem{O_3} concentrations.
As the increments are introduced by the TES assimilation, these vertical structures suggest that the tropospheric TES ¥chem{O_3} data have independent information for the lower and upper tropospheric ¥chem{O_3}. Jourdain et al. (2007) showed that the TES retrievals have 1--2 DOFs in the troposphere, with the largest DOFs for clear-sky scenes occurring at low latitudes where TES can distinguish between lower and upper tropospheric ¥chem{O_3}. The obtained analysis increments correspond well to the OmF in the control run at the same altitude (figure not shown), confirming that the data assimilation effectively reduced the model errors through the analysis steps.
Assimilation of other measurement generally provides much smaller increments on the tropospheric ¥chem{O_3}. The analysis increment varies largely with season and year, reflecting variations in short-term systematic model errors and observational constraints. After 2010 the availability of TES observations is strongly reduced, which explains the small increments in the later

years.

The mean analysis increment for ¥chem{NO_2} varies largely with space and time in the troposphere (not shown). For some regions with strong surface emissions, especially at NH mid-latitudes, the ¥chem{NO_2} increment becomes negative in the free troposphere because of the assimilation of non-¥chem{NO_2} measurements, compensating for the tropospheric ¥chem{NO_2} column changes caused by the (positive) surface emissions adjustment. This demonstrates that simultaneous data assimilation provides independent constraints on the surface emissions and free tropospheric ¥chem{NO_2} concentration, because of the use of observations from multiple species with different measurement sensitivities. Large adjustments are introduced to the ¥chem{NO_2} concentration in the UTLS, because the MLS ¥chem{O_3} and ¥chem{HNO_3} assimilation effectively corrects the model ¥chem{NO_2} bias as a~result of the correlations between species in the error covariance matrix.

¥section{Evaluation using independent observations}

¥subsection{¥chem{O_3}}

¥subsubsection{Ozonesonde}

The validation of the reanalysis and control run with global ozonesonde observations is summarised in Table~1. As depicted in Figs. 4 and 5, the CHASER simulation reproduced the observed main features of global ¥chem{O_3} distributions in the troposphere and lower stratosphere. However, there are systematic differences such as a~negative bias in the NH high latitude troposphere and a~positive bias from the middle troposphere to the lower stratosphere in the SH.

The reanalysis shows improved agreements with the ozonesonde observations. The mean negative bias in the NH high-latitudes is reduced in the troposphere. In the NH mid-latitudes, the model¥'s

positive bias in the UTLS and negative bias in the lower troposphere is mostly removed. The large reduction of the mean lower tropospheric bias in the NH mid-latitudes is attributed primarily to increased ¥chem{O_3} concentrations in boreal spring--summer (Fig.~5). The RMSEs compared with the ozonesonde observations are also reduced throughout the troposphere. The remaining errors, especially near the surface, are associated with low ~~measurement~~ retrieval sensitivities in the lower troposphere and gaps in the spatial representation between the model and observations.

In the tropics, the data assimilation generally increases the ¥chem{O_3} concentration, reducing the negative bias in the upper troposphere but increasing the positive bias in the lower troposphere. The increased positive bias could be attributed to the positive bias in the TES measurements (Sect.~7.2).

In the SH, the model's positive bias from the middle troposphere to the lower stratosphere is attributed largely to a~positive bias in the prescribed ¥chem{O_3} concentrations above 70¥,¥unit{hPa} in CHASER, which is mostly removed in the reanalysis. The observed seasonal and interannual variations are captured well in the reanalysis.

The observed tropospheric ¥chem{O_3} concentration shows variations from year to year during the reanalysis period (Fig.~5). As summarized in Table~2, the reanalysis reveals better agreements with the observed linear slope in most cases. The observed linear slope during the reanalysis period is positive ($+2.9 ¥pm 2.8$¥,¥unit{ppb¥,(8¥,years)^{-1}}) at the NH mid-latitudes between 850 and 500¥,¥unit{hPa}, but the significance of this trend is not very high. The slope over the eight-year period at the same region is also positive in the reanalysis data ($+1.2 ¥pm 2.1$¥,¥unit{ppb¥,(8¥,years)^{-1}}), whereas it is negative in the control run ($-1.2 ¥pm 2.1$¥,¥unit{ppb¥,(8¥,years)^{-1}}). At the NH mid-latitudes in the lower stratosphere (200--90¥,¥unit{hPa}), the observed slope is negative ($-17.7 ¥pm

41.9$¥,¥unit{ppb¥,(8¥,years)^{-1}}), whereas the reanalysis ($-25.7 ¥pm 38.8$¥,¥unit{ppb¥,(8¥,years)^{-1}}) shows better agreement with the observed slope than the control run ($-35.8 ¥pm 46.3$¥,¥unit{ppb¥,(8¥,years)^{-1}}). The seasonal and year-to-year variations are generally well reproduced in the control run in the NH troposphere (r¥,$=$¥,0.73--0.93), whereas the reanalysis further improves the temporal correlation by 0.07 between 850 and 500¥,¥unit{hPa} and by 0.04 between 500 and 200¥,¥unit{hPa} at the NH mid-latitudes.

The observed time series show obvious year-to-year variations in the tropics associated with variations such as in the El Ni¥'{n}o--Southern Oscillation (ENSO), including their influences on the biomass burning activity. The tropical ¥chem{O_3} variations are better represented in the reanalysis (r¥,$=$¥,0.80 between 850 and 500¥,¥unit{hPa} and r¥,$=$¥,0.72 between 500 and 200¥,¥unit{hPa}) than in the control run (r¥,$=$¥,0.74 and r¥,$=$¥,0.59). In the tropics and SH, annual and zonal mean ¥chem{O_3} concentration does not show clear linear trends during the reanalysis period either in the observations or reanalysis. However, local ¥chem{O_3} concentrations might have significant trends. For instance, Thompson et~al.~(2014) showed wintertime free tropospheric ¥chem{O_3} increases over Irene and R¥'{e}union probably due to that long-range transport of growing pollution in the SH. Further analyses will be required to investigate the detailed characteristics of ¥chem{O_3} variation.

The ozonesonde--analysis difference is slightly larger in 2010--2012 than in 2005--2009 (Table~3 and Fig.~6). The large positive bias throughout the troposphere in winter and negative bias below 500¥,¥unit{hPa} in spring--autumn remain in 2010--2012 (Fig.~6). This is associated with the decreased number of assimilation measurements (TES and OMI); this is discussed further in Sect.~7.3. In contrast, during 2005--2009 the mean ¥chem{O_3} bias does not change significantly with year in the reanalysis, which confirms the stable performance of the ¥chem{O_3} reanalysis field. Verstraeten et~al.~(2013) highlighted that the time series of the TES-sonde

¥chem{O_3} biases do not change over time, which suggests that TES is an appropriate instrument for long-term analysis of free tropospheric ¥chem{O_3}.

¥subsubsection{Aircraft}

Both the model and the reanalysis generally capture well the observed horizontal, vertical, and seasonal variations of ¥chem{O_3} concentration compared with the MOZAIC/IAGOS aircraft measurements (Figs. 7 and 8). However, the model mostly overestimates ¥chem{O_3} concentration from the northern tropics to the mid-latitudes and underestimates it at the NH high-latitudes in the middle and upper troposphere (between 850 and 300¥,¥unit{hPa} in Table~1), as consistently revealed by comparison with ozonesonde observations.

Although the improvement is not large in the upper troposphere (500--300 hPa, Fig. 7), ~~An~~ an improved agreement with the MOZAIC/IAGOS measurements is found in the reanalysis run in the middle troposphere (850--500¥,¥unit{hPa}) and at the aircraft--cruising altitude (300--200¥,¥unit{hPa}), as summarised in Table~1. M~~M~~ost of the negative bias of the model in the troposphere of the NH high latitudes is reduced throughout the reanalysis period. A~substantial improvement is observed at the aircraft--cruising altitude around the tropopause (between 300 and 200¥,¥unit{hPa}) at the NH high-latitudes ~~mainly because of the MLS assimilation~~; the mean positive bias is reduced from +8¥,{¥%} in the control run to +3¥,{¥%} in the reanalysis. By separately assimilating individual measurements through the Observing System Experiments (OSEs), we confirmed that the improvement is mainly attributed to the MLS assimilation (not shown).

From the NH subtropics to the mid-latitudes, the mean positive bias of the model at the aircraft--cruising altitude (300--200¥,¥unit{hPa}) is reduced, whereas the positive bias of low concentration in autumn--winter in the middle troposphere (850--500¥,¥unit{hPa}) is increased. In the tropics, the MOZAIC/IAGOS measurements were mostly collected near large biomass--burning areas (Fig.~7: e.g., Central

Africa and Southeast Asia), where ¥chem{O_3} concentration in the troposphere becomes too high in the reanalysis probably ~~attributing~~ attributed to a~positive bias in the TES ¥chem{O_3} observations (cf., Sect.~7.2). Note that more substantial improvements in comparison with the aircraft measurements are found in 2005--2009 than in the later years.

HIPPO measurements provide information on the vertical ¥chem{O_3} profiles over the Pacific. The observed tropospheric ¥chem{O_3} concentration is higher in the extratropics than the tropics, with higher concentrations in the NH than the SH (Fig.~9). The observed tropospheric ¥chem{O_3} concentration displays a~maximum in the NH subtropics in March (HIPPO3) because of the strong influence of stratospheric inflows along the westerly jet stream. The observed latitudinal-vertical distributions are generally captured well by both the model and the reanalysis for all the HIPPO campaigns.

The model shows negative biases in the NH extratropics and positive biases from the tropics to the SH compared with the HIPPO measurements (Table~1). These characteristics of the bias are commonly found in comparisons with global ozonesonde observations in this study (c.f., Section 5.1.1) and are reduced effectively in the reanalysis. A~considerable bias reduction can be found in the lower and middle tropospheric ¥chem{O_3} at the NH mid-latitudes where ¥chem{O_3} variations could be influenced by long-range transport from the Eurasian continent. Direct concentration adjustment by TES measurements in the troposphere and by MLS measurements in the UTLS played important roles in correcting tropospheric ¥chem{O_3} profiles. In addition, corrections made to the ¥chem{O_3} precursors emissions over the Eurasian continent by OMI, especially over East Asia, were important in influencing tropospheric ¥chem{O_3} concentration over the North Pacific around 35--60{¥degree}¥,N, especially in boreal spring. This demonstrates that the assimilation of multiple species data sets is a~powerful means by which to correct the global tropospheric ¥chem{O_3} profiles, including those over remote oceans. In contrast, the positive bias in

the tropics is further increased in the reanalysis (from +5¥,{¥%} in the control run to +8¥,{¥%} in the reanalysis between 850 and 500¥,¥unit{hPa} and from +10 to +15¥,{¥%} between 500 and 300¥,¥unit{hPa}), as mostly commonly found in comparisons against the MOZAIC/IAGOS and ozonesonde measurements (cf., Sects.~5.1.1 and 5.1.2).

Vertical profiles obtained during the NASA aircraft campaigns were also used to validate the ¥chem{O_3} profile (Fig.~10). The comparisons show improved agreements in the reanalysis in the middle and upper troposphere during INTEX-B over Mexico and during the ARCTAS campaign over the Arctic, but the model's positive bias near the surface is further increased for the INTEX-B profile. ~~,~~ For the DISCOVER-AQ profile, the model's negative bias in the free troposphere is mostly removed in the reanalysis. For the DC3 profiles, the model captures the observed tropospheric ¥chem{O_3} profiles well, whereas the assimilation leads to small overestimations.

¥subsection{CO}

¥subsubsection{Surface}

Surface ¥chem{CO} concentrations are compared with the WDCGG surface observations from 59 stations, as summarised in Table~4 and depicted for 12 selected stations in Fig.~11. The control run underestimates ¥chem{CO} concentration by up to about 60¥,¥unit{ppb} in the NH extratropics, with the largest negative bias in winter and smallest bias in summer. The model underestimation has been commonly found in most of the CTMs (Shindell et~al., 2006; Kopacz et~al., 2010; Fortems-Cheiney et~al., 2011; Stein et~al.,~2014). The model's negative bias is also found in most tropical sites, but not in the SH.

Most of the negative bias in the NH extratropics and in the tropics is removed in the reanalysis run, due to the increased surface ¥chem{CO} emissions in the analysis (cf., Sect.~6). The MOPITT assimilation

dominates the negative bias reduction through the surface ¥chem{CO} emission optimization, whereas the assimilation of other data has only a~small influence on the ¥chem{CO} concentration analysis through changes in the ¥chem{OH} field. The annual and regional mean surface bias becomes positive after assimilation at NH mid- and high-latitudes, which is illustrated at locations such as Midway and Bermuda (32{¥degree}¥,N, 65{¥degree}¥,W, figure not shown). The observed negative trends at most NH sites are captured well in the reanalysis.

Tropical ¥chem{CO} concentrations show district interannual variations associated with variations in tropical biomass-burning activities and meteorological conditions. The temporal correlations with the observations are about 0.1--0.2 higher in the reanalysis compared with the control run in the tropics at Christmas Island and Barbados.

In the SH, the model generally shows good agreement with the surface observations. However, assimilation increases the ¥chem{CO} concentration and leads to overestimations in some places (e.g., Showa). The mean negative bias at the SH mid-latitudes changed from $-$10¥,{¥%} in the control run to +7¥,{¥%} in the reanalysis.

¥subsubsection{Aircraft}

The model underestimates the ¥chem{CO} concentration in the tropics and the NH compared with the MOZAIC/IAGOS aircraft measurements throughout the troposphere (below 300¥,¥unit{hPa}) and around the tropopause at the aircraft--cruising altitude (between 300 and 200¥,¥unit{hPa}), as depicted in Fig.~12. The model's negative bias is mostly removed in the reanalysis, with a~mean improvement of 50--90¥,{¥%} throughout the troposphere, as summarised in Table~4. This confirms that the constraints provided for the surface emissions~~the emission constraints provided at the ground surface are~~ are propagated well into the concentrations of the entire troposphere with a~delay in the peak timing and decay in the amplitude~~.~~. Note that the CO concentrations were not

directly adjusted in the data assimilation. The spatial distribution in the upper troposphere is also captured well in the reanalysis (Fig.~7). Despite the overall improvement, the low concentrations in the NH lower and middle troposphere in summer and autumn remain underestimated, whereas the analysed concentration becomes too high in the NH high-latitudes at the aircraft-cruising altitude (Fig.~12). A~decreasing trend is observed in both the lower and upper troposphere in the NH, which is represented realistically in the reanalysis. The EDGAR 4.2 for 2008 was used for the model simulation for 2009--2012. The analysis and the comparison with the independent observations shows that this caused unrealistic interannual ¥chem{CO} variations and an underestimate of the decreasing trend in the control run.

The distinct interannual variations in the tropics (over Southeast Asia and around Central and North Africa) observed from the MOZAIC/IAGOS aircraft measurements mainly reflect variations in biomass-burning emissions. The temporal variations of ¥chem{CO} are captured better by the reanalysis between 850 and 500¥,¥unit{hPa} ($r=0.67$ in the control run and 0.78 in the reanalysis).

The HIPPO observations exhibit large latitudinal ¥chem{CO} gradients around 15--25{¥degree}¥,N over the Pacific for all campaigns (Fig.~13). Tropospheric air can be distinguished between the tropics and extratropics because of the transport barrier around the subtropical jet (Bowman, 2002; Miyazaki et~al., 2008). The transport barrier produces the large ¥chem{CO} gradient in the subtropics and acts to accumulate high levels of ¥chem{CO} in the NH extratropics. In the SH, ¥chem{CO} concentration increases with height in the free troposphere, because of the strong poleward transport in the upper troposphere from the tropics to the SH high-latitudes.

The assimilation increases ¥chem{CO} concentration and reduces the mean model negative bias by about 60--80¥,{¥%} in the NH extratropics against the HIPPO measurements. The remaining negative bias could be

attributed to overemphasised chemical destruction while air is transported from the Eurasian continent to the HIPPO locations over the central Pacific. For instance, the negative bias of the surface ¥chem{CO} concentration is mostly removed in the reanalysis over Yonaguni at the ground surface, located near (downwind of) large sources of Chinese emissions (Fig.~11). This suggests that the emission sources are realistically represented in the reanalysis. Errors in stratospheric ¥chem{CO} might also cause the negative bias through stratosphere--troposphere exchange (STE).

Reductions in the negative model bias of tropospheric ¥chem{CO} can be found in comparisons against the NASA aircraft campaign profiles from INTEX-B, ARCTAS-A, and DC3 (Fig.~10), although the bias reduction is small for the ARCTAS-B profile. Bian et~al.~(2013) demonstrated that most of the enhanced ¥chem{CO} concentrations observed during the ARCTAS-A~originate from Asian anthropogenic emissions. This suggests that the reanalysis realistically represent the Asian anthropogenic emissions and its influences on the Western Arctic ¥chem{CO} level. Bian et~al.~(2013) also suggested a~lower fraction of ¥chem{CO} from Asian anthropogenic emissions during the ARCTAS-B than during the ARCTAS-A~and showed that the along-track measurements are not representative of the concentrations within the large domain of the Western Arctic during the ARCTAS-B, which may explain the small bias reduction for the ARCTAS-B profile in our comparison. MOPITT data are assimilated equatorward of 65{¥degree}, and only the ¥chem{CO} emissions are optimised in the reanalysis. Direct adjustment of ¥chem{CO} concentration using high-latitude retrievals could be expected to improve the representation of ¥chem{CO} in the ARCTAS profiles, as demonstrated by Klonecki et~al.~(2012) using IASI measurements.

¥subsection{¥chem{NO_2}}

¥subsubsection{Tropospheric column}

Compared with the satellite retrievals, the model generally underestimates the ¥chem{NO_2} concentration over most industrial areas (e.g., East China, Europe, eastern USA, and South Africa) and over large biomass-burning areas (e.g., Central Africa), as shown by Fig.~14. The model underestimations are commonly found in comparisons against three different retrievals. The three products are produced using the same retrieval approach (Boersma et~al., 2011). Therefore, the overpass time difference and diurnal variations of chemical processes and emissions dominate the differences between these retrievals. The negative bias over these regions is greatly reduced in the reanalysis, decreasing the eight-year global mean negative bias by about 65, 45, and 30¥,{¥%} as compared with OMI, SCIAMACHY, and GOME-2, respectively (Table~5). The improvement can be also seen in the increased spatial correlation of 0.03--0.05 and in the reduced RMSE of 15--30¥,{¥%}.

Over East China, the model's negative bias is large in winter, whereas the assimilation reduces the wintertime bias by about 40¥,{¥%} compared with OMI retrievals. The observed low concentration in 2009 and high concentration in 2010--2012 are captured in the reanalysis, whereas the control run mostly failed to reproduce the interannual variability. The reanalysis shows larger positive trends than the control run, but the observed trend is even higher. The underestimation in the mean concentration and positive trend remain large in the reanalysis especially when compared with the SCIAMACHY and GOME-2 retrievals. Note that over polluted areas, realistic concentration pathways of ¥chem{NO_2} do not follow simple linear trends, but reflect a~combination of effects of environmental policies and economic activities. For instance, ¥chem{NO_x} emissions in China have been increasing because of the rapid economic growth, although an economic slowdown affected the growth rate in 2009 (Gu et~al., 2013).

Over Europe, the model's negative bias in summertime is reduced by about 10--30¥,{¥%} in the reanalysis. The observed wintertime concentration is high in 2011--2012 and relatively low in 2010 because

of the global economic recession and emission controls (Castellanos and Boersma, 2012). The assimilation increases the wintertime ¥chem{NO_2} concentration in 2011--2012 and captures the observed interannual variations better.

Over the eastern USA, the observed ¥chem{NO_2} concentration is high in 2005--2007 and low after 2008. The control run failed to reproduce these variations. In the reanalysis run, the model's negative bias is reduced in 2005--2007 compared with the OMI retrievals, showing a~negative trend in the reanalysis period. The improvement is smaller for the SCIAMACHY and GOME-2 retrievals.

Despite the general improvement, the reanalysis still has large negative biases compared with the satellite retrievals over the polluted regions. ~~One possible reason for the remaining underestimation of ¥chem{NO_2} concentrations is errors in model chemical equilibrium states.~~ There may be several reasons for the remaining underestimation of ¥chem{NO_2} concentrations. The analysis increment can partly be lost after the forecast because of the short lifetime of ¥chem{NO_x} (Miyazaki and Eskes 2013), especially when concentrations are adjusted. Other model processes, such as the diurnal cycle, boundary layer mixing and venting, and the chemical equilibrium at overpass may not be described well. Also, the averaging kernels show a relatively small sensitivity close to the surface, resulting in relatively smaller adjustments in the assimilation.~~The analysis increment can be lost quickly after the forecast because of the short lifetime of ¥chem{NO_x} (Miyazaki and Eskes, 2013).~~ The remaining bias varied considerably with season (e.g., the bias is mostly absent during summer over East China and the eastern USA), whereas the eight series of one-year calculations were conducted separately. Therefore, the remaining underestimation of ¥chem{NO_2} concentrations did not cause (spurious) gradual intra-annual and year-to-year increases in the estimated surface ¥chem{NO_x} emissions during the reanalysis period (cf., Sect.~6.1). The larger discrepancies with respect to the SCIAMACHY and GOME-2 retrievals may be attributed to the errors in the simulated diurnal ¥chem{NO_2} variations and a~bias between OMI and these retrievals. Both the emission factors and the tropospheric

concentrations of ¥chem{NO_x} are constrained only in the early afternoon by OMI, whereas no observational constraint on tropospheric ¥chem{NO_x} is available in the morning (i.e., during the SCIAMACHY and GOME-2 overpass time).

Over North Africa and Central Africa, the data assimilation removes most of the negative bias throughout the year, because of the increased biomass-burning emissions. The remaining negative bias in the reanalysis is relatively large when compared with the GOME-2 over North Africa and with SCIAMACHY and GOME-2 over Central Africa. The observed concentration is relatively small in 2010--2012 over North Africa, and the reanalysis captures the observed interannual variations better compared with the control run.

The control run fails to reproduce the observed distinct seasonal and interannual variations over Southeast Asia (r¥,$=$¥,0.74--0.79 in the control run and r¥,$=$¥,0.89--0.98 in the reanalysis compared with the three retrievals). The control run underestimates the concentration throughout the year with the largest biases in boreal spring in 2008--2009. The negative bias is greatly reduced in the reanalysis throughout the year, and the interannual variations are represented realistically. The remaining negative bias is large especially when compared with the GOME-2 retrievals.

¥subsubsection{Aircraft}

Compared with the vertical ¥chem{NO_2} profiles from the aircraft measurements, the simulated ¥chem{NO_2} concentration in the troposphere is generally too low (Fig.~10). For the ARCTAS profiles, the data assimilation has less impact in the troposphere. At high latitudes, the surface ¥chem{NO_x} emissions have only small effect on the tropospheric ¥chem{NO_2} profiles, and the observational error of the OMI measurements is large in comparison with the observed low concentration. Compared with the two DC3 profiles, the model is too high in the lower troposphere and too low in the middle/upper

troposphere. Data assimilation further increases the positive bias in the lower troposphere. The relatively coarse resolution of the model could cause large differences near the surface for comparisons at urban sites such as the DC3 profiles. Compared with the DISCOVER-AQ profile, the rapid change in ¥chem{NO_2} concentration in the lower troposphere is captured well by both the model and the reanalysis. The MLS ¥chem{O_3} and ¥chem{HNO_3} data assimilation effectively corrects the amount of ¥chem{NO_2} in the lower stratosphere, especially for the ARCTAS-A~profile, because of the use of the interspecies correlation in the analysis step and by influencing the ¥chem{NO_x}¥,$/$¥,¥chem{NO_y} species in the forecast step.

¥subsection{Other reactive species}

The observed main features of the ¥chem{HNO_3} profiles are captured by both the control and reanalysis runs. The increase in ¥chem{HNO_3} toward the surface is driven mainly by oxidation of ¥chem{NO_x} in polluted areas, which is visible in the INTEX-B, ARCTAS-B, DC3-DC8, DC3-GV, and DISCOVER-AQ profiles. The positive corrections by assimilation, primarily attributable to the increased ¥chem{NO_2} concentration and ¥chem{NO_x} emissions, reduce the model's underestimation for the DC3-GV profile, but led to concentrations that are too high for the INTEX-B, DC3-DC8, DC3-GV, and DISCOVER-AQ profiles. The assimilation only slightly influences the tropospheric ¥chem{HNO_3} concentration for the ARCTAS profiles because of the negligible impact of surface ¥chem{NO_x} emissions at NH high-latitudes and because of the absence of ¥chem{HNO_3} measurements for the troposphere. To improve further the lower tropospheric ¥chem{HNO_3} concentrations, corrections for its removal processes including depositions might be important. In the middle and upper troposphere, both the control and reanalysis runs generally underestimate ¥chem{HNO_3} concentration. The assimilation partly reduces the negative bias for the DC3 profiles. Additional positive increments of ¥chem{NO_2} appear required to compensate for the negative bias in ¥chem{HNO_3}. In the UTLS, the model ¥chem{HNO_3}

negative bias is reduced globally in the reanalysis because of the MLS assimilation. For the ARCTAS profiles, Liang et~al.~(2011) and Wespes et~al.~(2012) found that an adequate representation of stratospheric ¥chem{NO_y} inputs is important for the accurate simulation of tropospheric Arctic ¥chem{O_3} and ¥chem{NO_x} at pressures < 400¥,¥unit{hPa}.

The vertical ¥chem{HO_2} profile mainly reflects variations in water vapour concentrations in the troposphere, which decrease with latitude. The control run overestimates the tropospheric ¥chem{HO_2} concentration for the INTEX-B and ARCTAS-A~profiles, but underestimates it for the ARCTAS-B, DC3-DC8, and DC3-GV profiles. The reanalysis generally increases ¥chem{HO_2} concentrations, while it decreases~~ing~~ ¥chem{OH} concentration. The reaction of ¥chem{OH} with ¥chem{CO} converts ¥chem{OH} into ¥chem{HO_2}. Because of the increased ¥chem{CO} concentration, the assimilation increases the production of ¥chem{HO_2} in the NH. On the other hand, the ¥chem{HO_2}¥,$/$¥,¥chem{OH} ratio should decrease because of ¥chem{NO_x} increases which enhances the NO+¥chem{HO_2} and ¥chem{NO_2}+¥chem{HO_2} reactions. Further increase in ¥chem{NO_x} concentration is expected to reduce the ¥chem{HO_2} overestimation for the INTEX-B and ARCTAS-A~profiles. Errors in the removal of ¥chem{HO_2} by wet deposition processes might also cause biased concentrations.

Both the control and reanalysis runs overestimate the ¥chem{OH} concentration in the troposphere for the INTEX-B profile, but underestimate it for the ARCTAS and DC3 profiles. Data assimilation generally decreases the ¥chem{OH} concentration in the NH extratropics for the ARCTAS and DC3 profiles, corresponding to the increased concentration of ¥chem{CO}. For the INTEX-B profile, the data assimilation increases ¥chem{OH} and ¥chem{O_3} in the lower part of the troposphere because of the increased ¥chem{NO_x} emissions compensating the decrease due to ¥chem{CO}. Errors in the simulated ¥chem{H_2O} could also influence the performance of the simulation of

¥chem{OH} and ¥chem{HO_x}. Furthermore, large uncertainty in observed ¥chem{OH} concentrations also remains an important issue (e.g., Heard and Pilling, 2003; Stone et al., 2012).

The model captures the observed ¥chem{CH_2O} profiles in the troposphere well, but it generally underestimates the concentration. The reanalysis generally increases the ¥chem{CH_2O} concentration and reduces the negative bias of the model. However, its influence on the concentrations is small because of the lack of any direct measurement and the neglect of any interspecies correlation with ¥chem{CH_2O} in the reanalysis framework. Therefore, additional constraints from satellite measurements are required. Optimising isoprene emissions from ¥chem{CH_2O} measurements will be an important development (cf., Sect.~7.7).

Generally, these results reveal the positive benefit of the assimilation of multiple species data with different sensitivities on the analysis of unobserved species profiles in the troposphere and lower stratosphere. In particular, constraints obtained for the ¥chem{OH} profiles have a~large potential to influence the chemistry of the entire troposphere (cf., Sect.~7.4.2). However, many factors determine the overall analysis performance, such as chemical reaction rates, deposition rates, and atmospheric transports, which are hardly optimised by the currently available measurements.

¥section{Estimated emissions}

In previous publications (Miyazaki and Eskes, 2013; Miyazaki et~al., 2014) we demonstrated that the simultaneous analysis of chemical concentrations and emissions improves the estimate of surface ¥chem{NO_x} emissions and ¥chem{LNO_x} sources, with differences of up to 58¥,{¥%} in regional surface ¥chem{NO_x} emissions. The analysis increment produced directly via the chemical concentrations plays an important role in reducing the model--observation mismatches that arise from model errors other than those related to emissions. Here we

describe the estimated emissions briefly. Further detailed analyses of the eight-year variations in the estimated emission sources will be discussed in a~separate paper.

¥subsection{Surface ¥chem{NO_x} emissions}

The time series and global distributions of the analysed emission sources obtained during the reanalysis period are depicted in Figs. 15 and 16, respectively. The data assimilation increases the eight-year mean of global total surface ¥chem{NO_x} emissions from 38.4 to 42.2¥,¥unit{TgN}. The approximate 10¥,{¥%} increase of global total emissions is attributable to an approximate 7¥,{¥%} increase in the NH (20--90{¥degree}¥,N) and a~14¥,{¥%} increase in the tropics (20{¥degree}¥,S--20{¥degree}¥,N). The large increase of the NH emissions is associated with positive corrections over industrial areas such as China and India, and with corrections in Europe and the USA. Meanwhile, the increased emissions over Central Africa indicate larger emissions from biomass burning than shown by the inventories. These needed adjustments were commonly revealed by referring to our previous estimates for 2007 (Miyazaki and Eskes, 2013). The seasonal and interannual variability is also modified considerably in many regions. The emission inventories exhibit considerable uncertainties in representing seasonal and interannual emission variabilities associated with uncertain input information, such as economic conditions, biomass-burning activity, and emission factors (e.g., Jaegl¥'{e} et~al., 2005; Xiao et~al., 2010; Reuter et~al., 2014). For instance, the anthropogenic emissions were reported on a~yearly basis, and thus, seasonal variability in anthropogenic emissions such as from wintertime heating of buildings (e.g. Streets et~al., 2003) was not considered in the a~priori emissions. Wang et~al.~(2007) also suggested that the emission inventories largely underestimate soil emissions by a~factor of 2--3 at NH mid-latitudes during summer. The assumptions applied to the a~priori emissions (cf., Sect.~2.1; e.g., the anthropogenic emissions for 2008 are used in the estimations for 2009--2012) also cause an unrealistic lack of

interannual variability in the a~priori emissions and lead to significant differences between the a~priori and a~posteriori emissions.

¥subsection{¥chem{LNO_x} sources}

The average yearly global flash rate obtained for the reanalysis period 2005--2012 was 45.3¥,¥unit{flashes¥,s^{-1}}, which is comparable with climatological estimates of 46¥,¥unit{flashes¥,s^{-1}} derived from Lightning Imaging Sensor (LIS) and OTD measurements (Cecil et~al., 2014). The ¥chem{LNO_x} shows large discrepancies between the control and reanalysis runs. The mean annual global total ¥chem{LNO_x} source in the reanalysis run is estimated at 6.4¥,Tg¥,N for 2005--2012 and 6.0¥,Tg¥,N for 2005--2009, which is about 24 and 18¥,{¥%} higher than estimated from the parameterisation (5.1¥,Tg¥,N for both 2005--2009 and 2005--2012), respectively. The analysed ¥chem{LNO_x} sources show a~positive slope during 2005--2012 (+3.8¥,{¥%}¥,$¥pm$¥,4.2¥,¥unit{year^{-1}}) and enhanced sources during 2010--2012. From a~sensitivity reanalysis calculation that was performed by removing the TES measurements for 2005, we conclude that the large increase in 2010--2012 is at least partly introduced artificially because of the lack of constraints from the TES measurements. The TES data assimilation generally tends to decrease the global ¥chem{LNO_x} amount in the simultaneous assimilation framework (the global total ¥chem{LNO_x} source in 2005 is 5.8 and 6.6¥,Tg¥,N when estimated with and without the TES measurements, respectively). For the period 2005--2009, when the assimilated measurement density is nearly constant, the analysed ¥chem{LNO_x} variability is considered to be induced by variations in convective activity, thunderstorm type, and cloud distributions. The positive slope (+3.1¥,{¥%}¥,$¥pm$¥,4.2¥,¥unit{year^{-1}}) obtained for the period 2005--2009 in the reanalysis implies that variations in such processes led to the ¥chem{LNO_x} sources increase. The increase in the global ¥chem{LNO_x} sources for the period 2005--2009 is attributed to large increases over northern Africa

(+5.7¥,{¥%}¥,$¥pm$¥,26.8¥,¥unit{year^{-1}}), South America (+3.2¥,{¥%}¥,$¥pm$¥,22.0¥,¥unit{year^{-1}}), and the Atlantic Ocean (+7.4¥,{¥%}¥,$¥pm$¥,11.5¥,¥unit{year^{-1}}). Further detailed analyses are required to understand the possible causal mechanisms.

The global ¥chem{LNO_x} amount in the reanalysis (6.15¥,Tg¥,N) for 2007 is in agreement with our previous estimate (6.31¥,Tg¥,N) for the same year (Miyazaki et~al., 2014). However, because the tuning factor applied for the global total flash frequency is about 10¥,{¥%} larger than in the previous estimate based on the recent climatological estimates (Cecil et~al., 2014), the analysis increment can be different between the two estimates. For instance, the positive increment for 2007 is smaller or becomes negative over Siberia, Southeast Asia, and South America in the reanalysis. Note that the global structure of the analysis increment is generally similar between 2007 (figure not shown) and the eight-year reanalysis mean. Meanwhile, the seasonal variation of the tropical ¥chem{LNO_x} sources is modified more significantly in the reanalysis than in the previous estimate. In the reanalysis, the observational information is accumulated during the consequent one-year calculation after a~two-month spin-up, while continuously correcting the ¥chem{LNO_x} source factors. In the previous estimate (Miyazaki et~al., 2014), the ¥chem{LNO_x} sources were estimated from shorter data assimilation calculations (i.e., twelve 1¥,month calculations were conducted after a~15¥,day spin-up).

¥subsection{Surface ¥chem{CO} emissions}

The eight-year mean of global total emissions of ¥chem{CO} is increased by 36¥,{¥%} by data assimilation (1298 TgCO vs. 820 TgCO), attributable mainly to an approximate 110¥,{¥%} increase in the NH. The increase in the total ¥chem{CO} emission in the NH is large in the boreal late winter--spring, especially over China and Europe. Stein et~al.~(2014) commonly found it necessary to adjust emissions seasonally, using regionally varying scaling factors with

large corrections during winter--spring for industrialised countries. A~similar seasonality in the adjustments is found in Fig.~15, whereas the seasonality in the NH is mostly absent in the a~priori emissions. The positive increments for surface ¥chem{CO} emissions are introduced by assimilation of MOPITT ¥chem{CO} observations, whereas the assimilation of non-¥chem{CO} observations also affects the ¥chem{CO} emission estimation via changes in ¥chem{OH} concentrations. For instance, changes in surface ¥chem{NO_x} emissions decreased tropospheric ¥chem{OH} concentrations at NH mid-latitudes, and this in turn acted to increase the tropospheric ¥chem{CO} concentrations; this is discussed further in Sect.~7.4.2.

¥section{Discussion}

¥subsection{Impact of emission analysis}

The impact of the emission optimisation on the tropospheric ¥chem{O_3} analysis is evaluated based on comparison between the reanalysis run and a~sensitivity calculation that excludes the emission factors for the surface emissions and ¥chem{LNO_x} sources from the state vector. The emission optimisation influences the ¥chem{O_3} concentrations with mean changes of about 15¥,{¥%} in the tropics and 10¥,{¥%} in the NH mid-latitudes in the lower troposphere. These changes improve the agreement with ozonesonde observations in the lower troposphere in both the NH and SH (reanalysis v.s. w/o emission in Table~6), but not in the tropics. At the NH mid-latitudes the changes introduced by optimizing the emission factors improve the agreement with the ozonesonde observation from April to August below about 500¥,¥unit{hPa} (Fig.~17) associated with the pronounced ¥chem{O_3} production caused by ¥chem{NO_x} increases; the monthly mean positive bias below about 900 hPa is reduced by 10--15 ¥% in the summer and the negative bias between 900--500 hPa is reduced by 30--50 ¥% in spring and summer.~~the monthly mean negative bias is reduced by 30--50¥,{¥%}.~~ Vertical transport of ¥chem{O_3} and its precursors propagate the variations of surface emissions into the free troposphere, whereas the ¥chem{LNO_x} source

optimisation improves the performance of the upper tropospheric ¥chem{O_3} simulation directly. The impact of the emission optimization on the free troposphere is large throughout the year in the tropics.

The observed ¥chem{O_3} concentration in the NH mid-latitude between 850 and 500¥,¥unit{hPa} increased from 2005 to 2010 (+2.3¥,¥unit{ppb¥,(5¥,years)^{-1}}); the positive slope is represented in the reanalysis run (+1.0¥,¥unit{ppb¥,(5¥,years)^{-1}}), whereas a~case without emission source optimisation (w/o emission) shows a~negative slope ($-$1.1¥,¥unit{ppb¥,(5¥,years)^{-1}}). These results imply that the simultaneous optimisation approach improves the concentrations and emissions in the model and produces high-quality multiple-year reanalysis data for tropospheric ¥chem{O_3} profiles.

¥subsection{Biases in the observations}

TES ¥chem{O_3} retrievals are known to have positive bias compared with ozonesonde observations in the troposphere (e.g., Herman and Osterman, 2012; Verstraeten et~al., 2013). Based on systematic comparisons with ozonesonde observations, Verstraeten et~al.~(2013) determined that the upper and lower troposphere mean biases range from $-$0.4 to +13.3 and +3.9 to +6.0¥,¥unit{ppb}, respectively. In the reanalysis described in this paper we did not apply a~bias correction to TES because of the difficulty in estimating the bias structure that possibly varies temporally and spatially in the reanalysis period. We tested a~bias correction scheme with a~linear concentration--bias relationship, in which the slope and intercept estimated by Verstraeten et~al.~(2013) for five latitudinal bands of the upper troposphere (above 464¥,¥unit{hPa}), at 464¥,¥unit{hPa}, and for the lower troposphere (below 464¥,¥unit{hPa}) were interpolated in log-pressure to the model's vertical layers. For the Arctic lower troposphere, a~constant bias of 1.1¥,¥unit{ppb} was assumed because of the very small correlation found by Verstraeten et~al.~(2013). A~sensitivity calculation for the year 2005 with the

TES bias correction (TES-bias in Table~6) shows reductions in the positive ¥chem{O_3} bias in the tropical lower and middle troposphere against the ozonesonde observations. Conversely, in the NH mid- and high latitudes, the mean negative ¥chem{O_3} bias in the lower and middle troposphere increases. Because the bias was assumed constant with time, the representation of the interannual ¥chem{O_3} variation between 2005 and 2010 was not improved by applying the TES bias correction.

In the CHASER-DAS data assimilation approach, the ¥chem{O_3} analysis bias is not solely determined by bias in the assimilated ¥chem{O_3} measurements. A~sensitivity experiment without the assimilation of TES measurements (w/o TES in Table~6) shows improvements in the lower and middle tropospheric ¥chem{O_3} in the NH extratropics compared with the control run, demonstrating that the use of measurements other than TES measurements led to corrections in the lower and middle tropospheric ¥chem{O_3}. The additional use of the TES ¥chem{O_3} measurements further improved the ¥chem{O_3} analysis in most cases (see Table~6).

¥subsection{Satellite data availability}

Any discontinuities in the availability and coverage of the assimilated measurement will affect the quality of the reanalysis and estimated interannual variability. In particular, the number of assimilated TES ¥chem{O_3} retrievals decreases after 2010 through 2012, while approximately half of the OMI retrieval pixels per orbit are compromised since December~2009. Correspondingly, the data assimilation performance, as measured from the data assimilation statistics (Sect.~4) and comparisons against the independent observations (Sect.~5), became worse after 2010 in the NH. The lack of direct ¥chem{O_3} measurements and the reduced constraints from the precursor (i.e., ¥chem{NO_2}) measurements will degrade the ¥chem{O_3} analysis in the NH after 2010, and will also limit the evaluation of the analysis uncertainties (cf., Sect.~7.6) and may cause spurious

inter-annual changes and trends. Changes in the observing system thus limit the usability of the reanalysis for long-term variability studies.

¥subsection{Model bias}

¥subsubsection{A~priori emissions}

The choice of the a~priori emissions will influence the reanalysis result. To study the sensitivity of the reanalysis to the a~priori settings, emissions obtained from EDGAR-HTAP v2 (¥url{http://edgar.jrc.ec.europa.eu/htap_v2/index.php?SECURE=123}) for the years 2008 and 2010 were alternatively used as a~priori anthropogenic ¥chem{NO_x} and ¥chem{CO} emissions in the calculation for 2005 and 2010, respectively (the inventory was not provided for 2005 at the time of this study). EDGAR-HTAP v2 was produced using nationally reported emissions combined with regional scientific inventories from European Monitoring and Evaluation Programme (EMEP), Environmental Protection Agency (EPA), Greenhouse gas-Air Pollution Interactions and Synergies (GAINS), and Regional Emission Inventory in Asia (REAS). The model simulation using the a~priori emissions, constructed based on the EDGAR v4 and GFED v3 emissions, shows significant underestimations in tropospheric ¥chem{CO} concentrations, as in most of the CTMs (e.g., Stein et~al.,~2014), and this underestimation is large over urban sites in the NH (Sect.~5.2). The global ¥chem{CO} emissions of EDGAR-HTAP v2 inventory are about 20¥,{¥%} higher than the a~priori emissions. Using the EDGAR-HTAP v2 emissions instead of the a~priori emissions means that the negative bias in the simulated surface ¥chem{CO} concentration could be reduced by about 20--40¥,{¥%} in the tropics and the NH extratropics as is shown by the green lines in Fig.~11. The error reduction is large in winter--spring and small in summer in the NH and it is mostly negligible in the SH.

Despite the large differences in the simulated concentration, the

choice of a~priori emissions has only slight influence on the a~posteriori ¥chem{CO} concentrations and emissions. The annual global total emission is 1398 TgCO in the case with the EDGAR v4 and GFED v3 emissions and 1360 TgCO with the HTAP v2 emissions in 2005.

The ¥chem{O_3} analysis is only slightly influenced by the choice of a~priori emissions (reanalysis vs. HTAP in Table~6), except that the agreement against the ozonesonde observation is improved in the NH extratropics between 850 and 500¥,¥unit{hPa} through use of the EDGAR HTAP v2 emissions. The changes are attributable to the slightly different a~posteriori surface ¥chem{CO} and ¥chem{NO_x} emission (annual NH (20--90{¥degree}¥,N) total emission of 26.5¥,Tg¥,N in the case of the EDGAR v4 and GFED v3 emissions, and 29.4¥,Tg¥,N with the ~~HRAP~~ HTAP v2 emissions in 2005). The spatial distribution of the estimated ¥chem{LNO_x} sources is also somewhat influenced by the choice of a priori surface emissions in the NH mid-latitudes (not shown), which led to differences in the agreement with the ozonesonde observation in the upper troposphere at 200 hPa.

¥subsubsection{¥chem{OH} distribution}

¥chem{OH} is a~key driver of the tropospheric chemical system as the processes leading to the removal of hydrocarbons from the atmosphere starts with the reaction with OH. However, its distribution is represented poorly in CTMs. Patra et~al.~(2014) estimated an ¥text{NH}¥,$/$¥,¥text{SH} ¥chem{OH} ratio of $0.97 ¥pm 0.12$ with the help of methyl chloroform observations (a~proxy for ¥chem{OH} concentrations), whereas the ratio was estimated at 1.26 in the CHASER control run. The simulated ratio from this study falls within the range $1.28 ¥pm 0.10$ in the ACCMIP (the Atmospheric Chemistry and Climate Model Intercomparison Project) (Naik et~al., 2013). The concentration of ¥chem{OH} is directly linked to the concentrations of species determining the primary production (¥chem{O_3} and ¥chem{H_2O}), removal (¥chem{CO}, ¥chem{CH_4}) and regeneration of ¥chem{OH} (¥chem{NO_x}). Because the CHASER-DAS system constrains ¥chem{O_3}, ¥chem{CO} and ¥chem{NO_x}, this holds the promise of

a~positive impact on the modelled ¥chem{OH} concentration, given that the reactions are reasonably well described by the model. The impact of the assimilation on ¥chem{OH} is shown in Fig.~18.

The tropospheric ¥chem{OH} concentration is decreased by the assimilation in the NH and increased in the SH tropics; these changes are primarily attributable to the increased concentration of ¥chem{CO} and ¥chem{O_3}, respectively. From a~sensitivity experiment in which the state vector was modified (either the emission factors or the concentrations were excluded from the state vector), we confirmed that the emission optimisation solely decreases the ¥chem{OH} concentration in the NH troposphere, whereas both the concentration assimilation (mainly TES ¥chem{O_3}) and the emission optimization (mainly ¥chem{NO_x} emissions) increases the OH concentration in the tropics. The decrease of the tropospheric ¥chem{OH} concentration in the NH is found throughout the reanalysis period with the largest reductions of about 10¥,{¥%} during boreal spring--summer, leading to about 2¥,{¥%} decrease in the global annual mean ¥chem{OH} concentration linked to ¥chem{CO} increases in the NH. Changes in surface ¥chem{NO_x} emissions tend to decrease the annual mean tropospheric ¥chem{OH} concentration in the NH mid-latitudes by about 3¥,{¥%} and increase it in the tropics by about 5¥,{¥%}. The eight-year mean ¥text{NH}¥,$/$¥,¥text{SH} ¥chem{OH} ratio is 1.18 in the reanalysis, which is smaller than the values of 1.26 in the control run and 1.28 in the ACCMIP; the value of 1.18 is closer to the observational estimate (0.97) of Patra et~al.~(2014). Because the chemical lifetimes of ¥chem{NO_x} and ¥chem{CO} are affected by the amount of ¥chem{OH}, these changes once more suggest the importance of the simultaneous optimisation of the concentration and emissions on the entire tropospheric chemical system and the emission estimates.

Although the methyl chloroform analysis in Patra et~al.~(2014) has considerable uncertainties, the large discrepancy between the analysis of Patra et~al.~(2014) and our estimate suggests that possible errors in the modelled ¥chem{OH} could have had a~negative influence on the

reanalysis quality. If it is assumed that ¥chem{OH} is overestimated in the NH, then top-down emission estimates of reactive species such as ¥chem{CO} in the NH could also be overestimated. Sensitivity calculations were conducted to investigate the influence of the remaining possible ¥chem{OH} positive bias on the reanalysis results. In the sensitivity reanalysis calculations, a~factor of 0.8 was applied to the chemical reaction rate in the calculation of the chemical reaction ¥chem{CO} + ¥chem{OH} $¥to$ ¥chem{CO_2} + ¥chem{HO_2} for the NH, in consideration of the obtained difference (1.18 vs. 0.97). Other chemical reaction rates were not adjusted to simplify interpretation of the calculations. In the sensitivity model calculation with reduced ¥chem{OH}, the model's ¥chem{CO} negative bias is reduced by about 30--50¥,{¥%} in the NH. After assimilation with reduced ¥chem{OH}, the a~posteriori annual total ¥chem{CO} emissions become smaller by 15¥,{¥%} in the NH, whereas the a~posteriori ¥chem{CO} concentration at the surface does not change so obviously. Converserly, in the free troposphere, the a~posteriori ¥chem{CO} concentration becomes higher by about 5--10¥,{¥%} with the reduced ¥chem{OH}, which shows better agreement with the MOZAIC/IAGOS aircraft measurements. Thus, a~possible overestimation of the simulated ¥chem{OH} might lead to overestimations in the estimated ¥chem{CO} emissions and underestimations in the analysed ¥chem{CO} concentration in the free troposphere. The large positive adjustment needed for the ¥chem{CO} concentrations in the NH may therefore be related to deficiencies in the modelling of ¥chem{OH}, instead of too low emissions.

Note that ¥chem{CO} is produced by the oxidation of methane and biogenic non-methane hydrocarbons, a~process that contributes about half of the background ¥chem{CO} (Duncan et~al., 2007). This component can also account for part of the missing ¥chem{CO} concentrations. Stein et~al.~(2014) considered that anthropogenic ¥chem{CO} and VOC emissions in their inventory are too low for industrialised countries during winter and spring.

¥subsubsection{Other error sources}

The emissions of ¥chem{O_3} precursors other than ¥chem{NO_x} and ¥chem{CO}, such as VOCs, have a~pronounced influence on tropospheric chemistry. Further constraints are required to improve the ¥chem{O_3} analysis. Optimizing isoprene emissions from satellite ¥chem{CH_2O} measurements in the reanalysis framework have the potential to improve the ¥chem{O_3} analysis; this will be investigated in a~future study.

Incorrect model processes in atmospheric transport and chemistry lead to model forecast errors and degrade the reanalysis performance. Improving the forecast model is important for properly propagating observational information in space and among different species.

Meteorological fields used as inputs to the chemical reanalysis calculation were produced using an AGCM simulation nudged toward the meteorological reanalysis, in order to reproduce past meteorological variations while simulating the influence of sub-grid transport processes. Simultaneous assimilation of meteorological and chemical observations using an advanced data assimilation technique with consideration of radiative feedbacks and the covariances between the meteorological and chemical fields is expected to reduce systematic model errors and improve the chemical reanalysis performance.

¥subsection{Data assimilation setting}

To improve the data assimilation analysis with the limited ensemble size, covariance localisation was applied to neglect the error correlation among non- or weakly related variables in the background error covariance matrix. The inclusion of correlations between a~larger number of variables allows the propagation of observational information among various fields, but it requires a~large ensemble size to represent the multivariate relationships properly. For instance, Zoogman et~al.~(2014) demonstrated the possibility of

substantial benefit from joint ¥chem{O_3}--¥chem{CO} data assimilation in analysing near surface ¥chem{O_3}, if the instrument sensitivity for ¥chem{CO} in the boundary layer is larger than that for ¥chem{O_3}. Such covariances were not considered in our reanalysis calculation.

¥subsection{Uncertainty estimation}

Important information regarding the reanalysis product is provided by the error covariance. The analysis ensemble spread, which is estimated as the standard deviation of the simulated concentrations across the ensemble, in combination with the $¥chi^2$ test can be used as a~measure of the uncertainty of the reanalysis product within the EnKF assimilation framework (Miyazaki et~al., 2012b). The analysis spread is caused by errors in the model input data, model processes, and errors in the assimilated measurements, and it is reduced if the analysis converges to a~true state.

The analysis spread for ¥chem{O_3} is about 8--12¥,{¥%} relative to the analysed concentration in the tropical upper troposphere at 200¥,¥unit{hPa} (lower panels in Fig.~3), which is mostly determined by the assimilation of TES and MLS ¥chem{O_3} retrievals. The analysis spread is relatively small in the extratropical lower stratosphere (4--7¥,{¥%}) except at the polar regions, because of the high accuracy of the MLS measurements. At 700 and 400¥,¥unit{hPa}, the ¥chem{O_3} analysis spread is generally smaller in the tropics than the extratropics because of the higher sensitivities in the TES ¥chem{O_3} retrievals. The simultaneous emission and concentration optimisation is important in producing proper ensemble perturbations especially in the lower troposphere.

The global analysis spread for ¥chem{O_3} at 700 and 400¥,¥unit{hPa} is small in 2010--2012 (lower panels in Fig.~3). Considering the smaller level of agreement with the ozonesonde observations in 2010--2012 than in 2005--2009 (Table~3), the small analysis spread

cannot be regarded as an error reduction caused by the analysis converging to a~true state. The small analysis spread is likely associated with the lack of effective observations for measuring the analysis uncertainties and with the stiff chemical system. The obtained results indicate the requirements for additional observational information and/or stronger covariance inflation to the forecast error covariance for measuring the long-term analysis spread corresponding to actual analysis uncertainty. The too large $¥chi^2$ for OMI ¥chem{NO_2} and TES ¥chem{O_3} (Fig.~1) also suggested underestimations in the forecast error covariance in comparison with the actual OmF in 2010--2012 (cf., Sect.~4.1).

¥subsection{Applications and future developments}

The chemical reanalysis data set has great potential to contribute in a~number of ways to studies of the atmospheric environment and climate:

¥begin{enumerate}

¥item The concentration and emission data, which are produced consistently from a~single analysis system, provide comprehensive information on atmospheric composition variability, to improve the understanding of the processes controlling the atmospheric environment, including ¥chem{OH}, and their roles in changing climate.

¥item The reanalysis data provide initial and boundary conditions for climate and chemical simulations. They can be also used as an input to meteorological reanalyses for radiation calculations (Dragani and McNally, 2013).

¥item The obtained emission data can be used to study emission variabilities and to evaluate bottom-up emission inventories.

¥item The statistical information obtained during the reanalysis calculation can be used to suggest developments of models and

observations. The large spread can be regarded as an indicator for the requirement for further constraints, whereas the analysis increment identifies sources of model error.

¥end{enumerate}

Several further developments have been identified as necessary to improve the quality and value of the reanalysis data set:

¥begin{enumerate}

¥item Discontinuities in the assimilated measurements lead to changes in the reanalysis quality. The ¥chem{O_3} analysis performance was degraded in 2010--2012, corresponding to the decreased number of assimilated measurements. The influence of data discontinuities must be considered or removed when studying interannual variability and trends using products from reanalyses. Including more datasets such as from IASI and GOME-2 measurements could improve the reanalysis quality.

¥item Application of a~bias correction procedure for multiple measurements could improve the reanalysis quality but should be carefully checked (Inness et~al., 2013). Observations taken from aircraft and ozonesonde measurements or independent satellite datasets can be used as anchors in the bias correction. Alternatively, these data could be assimilated to provide additional unbiased constraints, as has been demonstrated by Baier et~al.~(2013).

¥item Additional constraints are required to improve the lower troposphere and boundary layer concentrations and emissions. Recently developed retrievals with high sensitivity to the lower troposphere would be helpful (e.g., Deeter et~al., 2013; Cuesta et~al., 2013). Moreover, the optimisation of additional precursors emissions could be important for improving the lower tropospheric analysis, including the representation of long-term variability.

¥item Extension of the forecast model to the entire stratosphere with

detailed stratospheric chemistry is expected to reduce forecast errors in both the stratosphere and the troposphere. We plan to replace the forecast model with one that has an updated chemical scheme and extended model top to the stratosphere (Watanabe et~al.,~2011). This would also allow the assimilation of total column measurements, in which the combined assimilation of limb profiles with nadir column measurements could benefit the reanalysis performance, especially in the UTLS (Barre et~al., 2013; Inness et~al., 2013; Emili et~al., 2014).

¥end{enumerate}

¥conclusions

We conducted a~chemical reanalysis calculation for the eight-years from 2005 to 2012 based on an assimilation of multiple satellite data sets obtained from OMI, MLS, TES, and MOPITT. The simultaneous optimisation of the chemical concentrations and the precursors emissions provides a~comprehensive data set that can be used for various applications in air-quality and climate research. By analysing simultaneously concentrations and emissions, the improved atmospheric concentrations of chemically-related species have the potential to improve the emission inversion, whereas the improved representations of the seasonal, interannual, and geographical variability of the emissions benefit the atmospheric concentration reanalysis through a~reduction in model forecast error.

Data assimilation statistics were analysed to evaluate the long-term stability of the chemical reanalysis. The analysis confirmed that the forecast error covariance was specified reasonably well. The OmFs without assimilation varied with year, which suggested an unrealistic lack of interannual variations in the precursor's emissions. The OmFs after assimilation became almost constant and decreased in the reanalysis, implying persistent reduction of model error and improved representation of emission variability. The information on the analysis uncertainty obtained during the assimilation adds value to

the chemical reanalysis data set, in which the observed large analysis spreads indicated a~requirement for further constraints from additional observations. However, the discontinuity in the assimilated measurements limited the usability of the reanalysis product. The number of available TES measurements decreased significantly after 2010, which produced unrealistically small analysis spreads and degraded the quality of the tropospheric ¥chem{O_3} analysis.

The analysed ¥chem{O_3}, ¥chem{CO}, ¥chem{NO_2} concentrations in the troposphere showed good agreement with independent observations on both regional and global scales, for seasonal and interannual variations from the lower troposphere to the lower stratosphere. The linear ozone slopes observed during the reanalysis period were positive at NH mid-latitudes in the lower troposphere and negative in the NH UTLS; these interannual variations were captured well in the reanalysis. The model simulation without any assimilation mostly failed to reproduce the observed variations. The simultaneous assimilation of multiple species data with optimisation of both the concentrations and emission fields was shown to be effective in correcting the profiles for the entire troposphere, including the long-term variations in ¥chem{O_3}, ¥chem{CO}, ¥chem{NO_2}. The global distribution of ¥chem{OH} was modified considerably, decreasing the difference between NH and SH because of the simultaneous assimilation throughout the reanalysis period, which played an important role in propagating observational information among various species and in modifying the chemical lifetimes of reactive gases. To conclude, the combined analysis of concentrations and emissions is considered an important development in tropospheric chemistry reanalysis.

To produce better chemical reanalysis data, it will be necessary to have additional constraints, a~better forecast model, and bias correction. Although the assimilation of multi-species data influences the representation of the entire chemical system, the influence of persistent model errors remains a~concern. For instance, the reanalysis still has large negative biases in ¥chem{NO_2} concentrations over the polluted regions, which may be associated with errors in for

instance the model chemical equilibrium states, planetary boundary layer (PBL) mixing, and diurnal variations of chemical processes and emissions. ~~.~~Adjusting additional model parameters such as VOC emissions, deposition, and/or chemical reactions rates by adding observational constraints will help to reduce model errors. An extension of the forecast model to the entire stratosphere and incorporating detailed stratospheric chemistry is expected to reduce forecast errors in both the stratosphere and troposphere and allow the assimilation of total column measurements (Inness et~al., 2013). Techniques to reduce the influence of discontinuities in the assimilated measurements and to use sparse observations efficiently (van der A~et~al., 2010) on the quality of the reanalysis are also required.

¥begin{acknowledgements}
We acknowledge the free use of tropospheric ¥chem{NO_2} column data from the SCIAMACHY, GOME-2, and OMI sensors from ¥url{www.temis.nl}.
We also acknowledge the use of data products from the NASA aircrafts, the MOZAIC/IAGOS programmes, and the AURA and EOS Terra satellite missions. We would also like to thank the two anonymous reviewers for their valuable comments.
This work was supported by the JSPS KAKENHI Grant Numbers 24740327 and 25241006.
¥end{acknowledgements}

¥begin{thebibliography}{00}

¥bibitem{1}
Baier,~F., Erbertseder,~T., Elbern,~H., and Schwinger,~J.: Impact of different ozone sounding networks on a~4D-Var stratospheric data assimilation system,~Q. J. Roy. Meteor. Soc., 139, 2055--2067, doi:¥href{http://dx.doi.org/10.1002/qj.2086}{10.1002/qj.2086}, 2013.

¥bibitem{2}
Barr¥'{e},~J., Peuch,~V.-H., Lahoz,~W., Attie,~J.-L., Josse,~B., Piacentini,~A., Eremenko,~M., Dufour,~G., Nedelec,~P., von Clarmann,~T., and El Amraoui,~L.: Combined data assimilation of ozone tropospheric columns and stratospheric profiles in a~high-resolution CTM,~Q. J. Roy. Meteor. Soc., 140, 966--981, doi:¥href{http://dx.doi.org/10.1002/qj.2176}{10.1002/qj.2176}, 2013.

¥bibitem{3}
Barth, M. C., Cantrell, C. A., Brune, W. H., Rutledge, S. A., Crawford, J. H., Huntrieser, H., Carey, L. D., MacGorman, D., Weisman, M., Pickering, K. E., Bruning, E., Anderson, B., Apel, E., Biggerstaff, M., Campos, T., Campuzano-Jost, P., Cohen, R., Crounse, J., Day, D. A., Diskin, G., Flocke, F., Fried, A., Garland, C., Heikes, B., Honomichl, S., Hornbrook, R., Huey, L. G., Jimenez, J. L., Lang, T., Lichtenstern, M., Mikoviny, T., Nault, B., O'Sullivan, D., Pan, L. L., Peischl, J., Pollack, I., Richter, D., Riemer, D., Ryerson, T., Schlager, H., St. Clair, J., Walega, J., Weibring, P., Weinheimer, A., Wennberg, P., Wisthaler, A., Wooldridge, P. J., and Ziegler, C.: The Deep Convective Clouds and Chemistry (DC3) field campaign, B. Am. Meteorol. Soc., online first, ¥doi{10.1175/BAMS-D-13-00290.1}, 2015.

¥bibitem{4}
Beer,~R.: TES on the Aura mission: scientific objectives, measurements, and analysis overview, IEEE~T. Geosci. Remote, 44, 1102--1105, 2006.

¥bibitem{6S}
Bian,~H., Colarco,~P.~R., Chin,~M., Chen,~G., Rodriguez,~J.~M., Liang,~Q., Blake,~D., Chu,~D.~A., da~Silva,~A., Darmenov,~A.~S., Diskin,~G., Fuelberg,~H.~E., Huey,~G., Kondo,~Y., Nielsen,~J.~E., Pan,~X., and Wisthaler,~A.: Source attributions of pollution to the Western Arctic during the NASA ARCTAS field campaign, Atmos. Chem. Phys., 13, 4707--4721, doi:¥href{http://dx.doi.org/10.5194/acp-13-4707-2013}{10.5194/acp-13-4707-2013}, 2013.

¥bibitem{5S}
Boersma,~K.~F., Eskes,~H.~J., Dirksen,~R.~J., van~der~A,~R.~J., Veefkind,~J.~P., Stammes,~P., Huijnen,~V., Kleipool,~Q.~L., Sneep,~M., Claas,~J., Leit¥~{a}o,~J., Richter,~A., Zhou,~Y., and Brunner,~D.: An improved tropospheric NO$_{2}$ column retrieval algorithm for the Ozone Monitoring Instrument, Atmos. Meas. Tech., 4, 1905--1928, doi:¥href{http://dx.doi.org/10.5194/amt-4-1905-2011}{10.5194/amt-4-1905-2011}, 2011.

¥bibitem{7}
Bovensmann,~H., Burrows,~J.~P., Buchwitz,~M., Frerick,~J., No¥"{e}l,~S., Rozanov,~V.~V., Chance,~K.~V., and Goede,~A.~P.~H.: SCIAMACHY: mission objectives and measurement modes,~J.~Atmos. Sci., 56, 127--150, 1999.

¥bibitem{8}
Bowman,~K.~P. and Carrie,~G.~R.: The mean-meridional transport circulation of the troposphere in an idealized GCM,~J. Atmos. Sci., 59, 1502--1514, 2002.

¥bibitem{9}
Callies,~J., Corpaccioli,~E., Eisinger,~M., Hahne,~A., and Lefebvre,~A.: GOME-2 -- MetOp's second generation sensor for operational ozone monitoring, ESA Bull.-Eur. Space, 102, 28--36, 2000.

¥bibitem{10}
Castellanos,~P. and Boersma,~K.~F.: Reductions in nitrogen oxides over Europe driven by environmental policy and economic recession, Sci. Rep., 2, 265, doi:¥href{http://dx.doi.org/10.1038/srep00265}{10.1038/srep00265}, 2012.

¥bibitem{11}
Cecil,~D.~J., Buechler,~D.~E., and Blakeslee,~R.~J.: Gridded lightning climatology from TRMM-LIS and OTD: dataset description, Atmos. Res., 135--136, 404--414, 2014.

¥bibitem{12S}
Coman,~A., Foret,~G., Beekmann,~M., Eremenko,~M., Dufour,~G., Gaubert,~B., Ung,~A., Schmechtig,~C., Flaud,~J.-M., and Bergametti,~G.: Assimilation of IASI partial tropospheric columns with an Ensemble Kalman Filter over Europe, Atmos. Chem. Phys., 12, 2513--2532, doi:¥href{http://dx.doi.org/10.5194/acp-12-2513-2012}{10.5194/acp-12-2513-2012}, 2012.

¥bibitem{13}
Constantinescu,~E., Sandu,~A., Chai,~T., and Carmichael,~G.: Ensemble-based chemical data assimilation. Part I: General approach,~Q. J. Roy. Meteor. Soc., 133, 1229--1243, 2007.

¥bibitem{14S}
Crumeyrolle,~S., Chen,~G., Ziemba,~L., Beyersdorf,~A., Thornhill,~L., Winstead,~E., Moore,~R.~H., Shook,~M.~A., Hudgins,~C., and Anderson,~B.~E.: Factors that influence surface PM$_{2.5}$ values inferred from satellite observations: perspective gained for the US Baltimore--Washington metropolitan area during DISCOVER-AQ, Atmos. Chem. Phys., 14, 2139--2153, doi:¥href{http://dx.doi.org/10.5194/acp-14-2139-2014}{10.5194/acp-14-2139-2014}, 2014.

¥bibitem{15S}

Cuesta,~J., Eremenko,~M., Liu,~X., Dufour,~G., Cai,~Z., H¥"{o}pfner,~M., von~Clarmann,~T., Sellitto,~P., Foret,~G., Gaubert,~B., Beekmann,~M., Orphal,~J., Chance,~K., Spurr,~R., and Flaud,~J.-M.: Satellite observation of lowermost tropospheric ozone by multispectral synergism of IASI thermal infrared and GOME-2 ultraviolet measurements over Europe, Atmos. Chem. Phys., 13, 9675--9693, doi:¥href{http://dx.doi.org/10.5194/acp-13-9675-2013}{10.5194/acp-13-9675-2013}, 2013.

¥bibitem{16}
Deeter,~M.~N., Martinez-Alonso,~S., Edwards,~D.~P., Emmons,~L.~K., Gille,~J.~C., Worden,~H.~M., Pittman,~J.~V., Daube,~B.~C., and Wofsy,~S.~C.: Validation of MOPITT Version 5 thermal-infrared, near-infrared, and multispectral carbon monoxide profile retrievals for 2000--2011,~J. Geophys. Res.-Atmos., 118, 6710--6725, doi:¥href{http://dx.doi.org/10.1002/jgrd.50272}{10.1002/jgrd.50272}, 2013.

¥bibitem{17}
Dragani,~R. and McNally,~A.~P.: Operational assimilation of ozone-sensitive infrared radiances at ECMWF,~Q. J. Roy. Meteor. Soc., 139, 2068--2080, doi:¥href{http://dx.doi.org/10.1002/qj.2106}{10.1002/qj.2106}, 2013.

¥bibitem{18}
Duncan,~B.~N., Logan,~J.~A., Bey,~I., Megretskaia,~I.~A., Yantosca,~R.~M., Novelli,~P.~C., Jones,~N.~B., and Rinsland,~C.~P.: The global budget of CO, 1988--1997: source estimates and validation with a~global model,~J. Geophys. Res., 112, D22301, doi:¥href{http://dx.doi.org/10.1029/2007JD008459}{10.1029/2007JD008459}, 2007.

¥bibitem{19S}
Emili,~E., Barret,~B., Massart,~S., Le~Flochmoen,~E., Piacentini,~A., El~Amraoui,~L., Pannekoucke,~O., and Cariolle,~D.: Combined assimilation of IASI and MLS observations to constrain tropospheric and stratospheric ozone in a global chemical transport model, Atmos. Chem. Phys., 14, 177--198, doi:¥href{http://dx.doi.org/10.5194/acp-14-177-2014}{10.5194/acp-14-177-2014}, 2014.

¥bibitem{20S}
Eskes,~H.~J. and Boersma,~K.~F.: Averaging kernels for DOAS total-column satellite retrievals, Atmos. Chem. Phys., 3, 1285--1291, doi:¥href{http://dx.doi.org/10.5194/acp-3-1285-2003}{10.5194/acp-3-1285-2003}, 2003.

¥bibitem{21S}
Flemming,~J., Inness,~A., Jones,~L., Eskes,~H.~J., Huijnen,~V., Schultz,~M.~G., Stein,~O., Cariolle,~D., Kinnison,~D., and Brasseur,~G.: Forecasts and assimilation experiments of the Antarctic ozone hole 2008, Atmos. Chem. Phys., 11, 1961--1977, doi:¥href{http://dx.doi.org/10.5194/acp-11-1961-2011}{10.5194/acp-11-1961-2011}, 2011.

¥bibitem{22}
Fortems-Cheiney,~A., Chevallier,~F., Pison,~I., Bousquet,~P., Szopa,~S., Deeter,~M.~N., and Clerbaux,~C.: Ten years of CO emissions as seen from Measurements of Pollution in the Troposphere (MOPITT),~J.~Geophys. Res., 116, D05304, ¥doi{10.1029/2010JD014416}, 2011.

¥bibitem{23}
Graedel,~T.~E., Bates,~T.~S., Bouwman,~A.~F., Cunnold,~D., Dignon,~J., Fung,~I., Jacob,~D.~J., Lamb,~B.~K., Logan,~J.~A., Marland,~G., Middleton,~P., Pacyna,~J.~M., Placet,~M., and Veldt,~C.: A~compilation of inventories of emissions to the atmosphere, Global Biogeochem. Cy., 7, 1--26, 1993.

¥bibitem{24}
Gu,~D., Wang,~Y., Smeltzer,~C., and Liu,~Z.: Reduction in ¥chem{NO_x} emission trends over China: regional and seasonal variations, Environ. Sci. Technol., 47, 12912--12919, doi:¥href{http://dx.doi.org/10.1021/es401727e}{10.1021/es401727e}, 2013.

¥bibitem{26}
Hains,~J.~C., Boersma,~K.~F., Kroon,~M., Dirksen,~R.~J., Cohen,~R.~C., Perring,~A.~E., Bucsela,~E., Volten,~H., Swart,~D.~P.~J., Richter,~A., Wittrock,~F., Schoenhardt,~A., Wagner,~T., Ibrahim,~O.~W., van Roozendael,~M., Pinardi,~G., Gleason,~J.~F., Veefkind,~J.~P., and Levelt,~P.: Testing and improving OMI DOMINO tropospheric ¥chem{NO_2} using observations from the DANDELIONS and NTEX-B validation campaigns,~J. Geophys. Res.-Atmos., 115, D05301, doi:¥href{http://dx.doi.org/10.1029/2009JD012399}{10.1029/2009JD012399}, 2010.

¥bibitem{27}
Heald,~C.~L., Jacob,~D.~J., Jones,~D.~B.~A., Palmer,~P.~I., Logan,~J.~A., and Streets,~D.~G.: Comparative inverse analysis of satellite (MOPITT) and aircraft (TRACE-P) observations to estimate Asian sources of carbon monoxide,~J.~Geophys. Res., 109, D23306, ¥doi{10.1029/2004JD005185}, 2004.

¥bibitem{28}

Heard,~D.~E. and Pilling,~M.~J.: Measurement of ¥chem{OH} and ¥chem{HO_2} in the troposphere, Chem. Rev., 103, 5163--5198, 2003.

¥bibitem{29}
Herman,~R.~L. and Kulawik,~S.~S. (eds.): Tropospheric Emission Spectrometer TES Level 2 (L2) Data User's Guide, D-38042, version 5.0, Jet Propulsion Laboratory, California Institute of Technology, Pasadena, CA, available at: ¥url{http://tes.jpl.nasa.gov/documents} (last access: 10~January~2015), 2013.

¥bibitem{30}
Herman,~R.~L. and Osterman,~G.~B. (Eds.): Tropospheric Emission Spectrometer Data Validation Report (Version F06¥_08, F06¥_09 data), D-33192, Version 5.0, Jet Propulsion Laboratory, California Institute of Technology, Pasadena, CA, available at: ¥url{https://eosweb.larc.nasa.gov/project/tes/validation} (last access: 10~January~2015), 2012.

¥bibitem{31S}
Hooghiemstra,~P.~B., Krol,~M.~C., Meirink,~J.~F., Bergamaschi,~P., van~der~Werf,~G.~R., Novelli,~P.~C., Aben,~I., and R¥"{o}ckmann,~T.: Optimizing global CO emission estimates using a four-dimensional variational data assimilation system and surface network observations, Atmos. Chem. Phys., 11, 4705--4723, doi:¥href{http://dx.doi.org/10.5194/acp-11-4705-2011}{10.5194/acp-11-4705-2011}, 2011.

¥bibitem{32}
HTAP 2010: Part A: Ozone and Particulate Matter, edited by: Dentener,~F., Keating,~T., and Akimoto,~H., prepared by the Task Force on Hemispheric Transport of Air Pollution acting within the framework of the Convention on Long-range Transboundary Air Pollution, United Nations, New York and Geneva,

2010.

¥bibitem{33}
Hunt,~B.~R., Kostelich,~E.~J., and Szunyogh,~I.: Efficient data assimilation for spatiotemporal chaos: a~local ensemble transform Kalman filter, Physica D, 230, 112--126, 2007.

¥bibitem{34S}
Inness,~A., Baier,~F., Benedetti,~A., Bouarar,~I., Chabrillat,~S., Clark,~H., Clerbaux,~C., Coheur,~P., Engelen,~R.~J., Errera,~Q., Flemming,~J., George,~M., Granier,~C., Hadji-Lazaro,~J., Huijnen,~V., Hurtmans,~D., Jones,~L., Kaiser,~J.~W., Kapsomenakis,~J., Lefever,~K., Leit¥~{a}o,~J., Razinger,~M., Richter,~A., Schultz,~M.~G., Simmons,~A.~J., Suttie,~M., Stein,~O., Th¥'{e}paut,~J.-N., Thouret,~V., Vrekoussis,~M., Zerefos,~C., and the~MACC~team: The MACC reanalysis: an 8¥,yr data set of atmospheric composition, Atmos. Chem. Phys., 13, 4073--4109, doi:¥href{http://dx.doi.org/10.5194/acp-13-4073-2013}{10.5194/acp-13-4073-2013}, 2013.

¥bibitem{35}
IPCC: Climate Change 2013: the Physical Science Basis, contribution of Working Group I to the Fifth Assessment Report of the Intergovernmental Panel on Climate Change, edited by: Stocker,~T.~F., Qin,~D., Plattner,~G.-K., Tignor,~M., Allen,~S.~K., Boschung,~J., Nauels,~A., Xia,~Y., Bex,~V., and Midgley,~P.~M., Cambridge University Press, Cambridge, UK and New York, NY, USA, 1535 pp., doi:¥href{http://dx.doi.org/10.1017/CBO9781107415324}{10.1017/CBO9781107415324}, 2013.

¥bibitem{36}

Jackson,~D.~R.: Assimilation of EOS MLS ozone observations in the Met Office data-assimilation system,~Q. J. Roy. Meteor. Soc., 133, 1771--1788, doi:¥href{http://dx.doi.org/10.1002/qj.140}{10.1002/qj.140}, 2007.

¥bibitem{37S}
Jacob,~D.~J., Crawford,~J.~H., Maring,~H., Clarke,~A.~D., Dibb,~J.~E., Emmons,~L.~K., Ferrare,~R.~A., Hostetler,~C.~A., Russell,~P.~B., Singh,~H.~B., Thompson,~A.~M., Shaw,~G.~E., McCauley,~E., Pederson,~J.~R., and Fisher,~J.~A.: The Arctic Research of the Composition of the Troposphere from Aircraft and Satellites (ARCTAS) mission: design, execution, and first results, Atmos. Chem. Phys., 10, 5191--5212, doi:¥href{http://dx.doi.org/10.5194/acp-10-5191-2010}{10.5194/acp-10-5191-2010}, 2010.

¥bibitem{38}
Jaegl¥'{e},~L., Steinberger,~L., Martin,~R.~V., and Chance,~K.: Global partitioning of ¥chem{NO_x} sources using satellite observations: relative roles of fossil fuel combustion, biomass burning and soil emissions, Faraday Discuss., 130, 407--423, 2005.

¥bibitem{90}

Jourdain, L., Worden, H. M., Bowman, K., Li, Q. B., Eldering, A., Kulawik, S. S., Osterman, G., Boersma, K. F., Fisher, B., Rins- land, C. P., Beer, R., and Gunson, M.: Tropospheric vertical distribution of tropical Atlantic ozone observed by TES during the northern African biomass burning season, Geophys. Res. Lett., 34, L04810, doi:10.1029/2006GL028284, 2007.

¥bibitem{39}
Kanamitsu,~M., Ebisuzaki,~W., Woollen,~J., Yang,~S.~K., Hnilo,~J.~J., Fiorino,~M., and Potter,~G.~L.: NCEP-DOE AMIP-II reanalysis (R-2),~B. Am. Meteorol. Soc., 83, 1631--1643,

doi:¥href{http://dx.doi.org/10.1175/BAMS-83-11-1631}{10.1175/BAMS-83-11-1631},
2002.

¥bibitem{40}
Kalnay,~E.: Atmospheric Modeling, Data Assimilation and Predictability,
Cambridge University Press, 341 pp., 2003.

¥bibitem{25}
Kiesewetter,~G., Sinnhuber,~B.~M., Vountas,~M., Weber,~M., and
Burrows,~J.~P.: A~long-term stratospheric ozone data set from assimilation of
satellite observations: high-latitude ozone anomalies,~J. Geophys. Res., 115,
D10307,
doi:¥href{http://dx.doi.org/10.1029/2009JD013362}{10.1029/2009JD013362},
2010.

¥bibitem{41S}
Klonecki,~A., Pommier,~M., Clerbaux,~C., Ancellet,~G., Cammas,~J.-P.,
Coheur,~P.-F., Cozic,~A., Diskin,~G.~S., Hadji-Lazaro,~J.,
Hauglustaine,~D.~A., Hurtmans,~D., Khattatov,~B., Lamarque,~J.-F.,
Law,~K.~S., Nedelec,~P., Paris,~J.-D., Podolske,~J.~R., Prunet,~P.,
Schlager,~H., Szopa,~S., and Turquety,~S.: Assimilation of IASI satellite CO
fields into a global chemistry transport model for validation against
aircraft measurements, Atmos. Chem. Phys., 12, 4493--4512,
doi:¥href{http://dx.doi.org/10.5194/acp-12-4493-2012}{10.5194/acp-12-4493-2012},
2012.

¥bibitem{42S}
Kopacz,~M., Jacob,~D.~J., Fisher,~J.~A., Logan,~J.~A., Zhang,~L.,
Megretskaia,~I.~A., Yantosca,~R.~M., Singh,~K., Henze,~D.~K., Burrows,~J.~P.,
Buchwitz,~M., Khlystova,~I., McMillan,~W.~W., Gille,~J.~C., Edwards,~D.~P.,

Eldering,~A., Thouret,~V., and Nedelec,~P.: Global estimates of CO sources with high resolution by adjoint inversion of multiple satellite datasets (MOPITT, AIRS, SCIAMACHY, TES), Atmos. Chem. Phys., 10, 855--876, doi:¥href{http://dx.doi.org/10.5194/acp-10-855-2010}{10.5194/acp-10-855-2010}, 2010.

¥bibitem{43}
Lahoz,~W.~A. and Schneider,~P.: Data assimilation: making sense of Earth Observation, Frontiers in Environmental Science, 2, 16, doi:¥href{http://dx.doi.org/10.3389/fenvs.2014.00016}{10.3389/fenvs.2014.00016}, 2014.

¥bibitem{44}
Lamsal,~L.~N., Martin,~R.~V., van Donkelaar,~A., Celarier,~E.~a., Bucsela,~E.~J., Boersma,~K.~F., Dirksen,~C.~L., and Wang,~Y.: Indirect validation of tropospheric nitrogen dioxide retrieved from the OMI satellite instrument: insight into the seasonal variation of nitrogen oxides at northern midlatitudes,~J.~Geophys. Res., 115, 1--15, 2010.

¥bibitem{46}
Levelt,~P.~F., Hilsenrath,~E., Leppelmeier,~G.~W., van den Oord,~G.~H.~J., Bhartia,~P.~K., Tamminen,~J., de Haan,~J.~F., and Veefkind,~J.~P.: Science objectives of the Ozone Monitoring Instrument, Geosci. Remote Sens., 44, 1199--1208, 2006.

¥bibitem{45}
Levy,~H.: Normal atmosphere: large radical and formaldehyde concentrations predicted, Science, 173, 141--143, 1971.

¥bibitem{47S}
Liang,~Q., Rodriguez,~J.~M., Douglass,~A.~R., Crawford,~J.~H., Olson,~J.~R., Apel,~E., Bian,~H., Blake,~D.~R., Brune,~W., Chin,~M., Colarco,~P.~R., da~Silva,~A., Diskin,~G.~S., Duncan,~B.~N., Huey,~L.~G., Knapp,~D.~J., Montzka,~D.~D., Nielsen,~J.~E., Pawson,~S., Riemer,~D.~D., Weinheimer,~A.~J., and Wisthaler,~A.: Reactive nitrogen, ozone and ozone production in the Arctic troposphere and the impact of stratosphere-troposphere exchange, Atmos. Chem. Phys., 11, 13181--13199, doi:¥href{http://dx.doi.org/10.5194/acp-11-13181-2011}{10.5194/acp-11-13181-2011}, 2011.

¥bibitem{48}
Livesey,~N.~J., Read,~W.~G., Froidevaux,~L., Lambert,~A., Manney,~G.~L., Pumphrey,~H.~C., Santee,~M.~L., Schwartz,~M.~J., Wang,~S., Cofield,~R.~E., Cuddy,~D.~T., Fuller,~R.~A., Jarnot,~R.~F., Jiang,~J.~H., Knosp,~B.~W., Stek,~P.~C., Wagner,~P.~A., and Wu,~D.~L.: Aura Microwave Limb Sounder (MLS), Version 3.3 Level 2 data quality and description document, Tech. Rep. JPL D-33509, Jet Propul. Lab., Pasadena, CA, 2011.

¥bibitem{49}
Logan,~J.~A., Prather,~M.~J., Wofsy,~S.~C., and McElroy,~M.~B.: Tropospheric chemistry: a~global perspective,~J. Geophys. Res., 86, 7210--7354, 1981.

¥bibitem{50}
Martin,~R.~V., Sauvage,~B., Folkins,~I., Sioris,~C.~E., Boone,~C., Bernath,~P., and Ziemke,~J.~R.: Space-based constraints on the production of nitric oxide by lightning,~J. Geophys. Res., 112, D09309, doi:¥href{http://dx.doi.org/10.1029/2006JD007831}{10.1029/2006JD007831}, 2007.

¥bibitem{51}

M¥"{e}nard,~R. and Chang,~L.-P.: Assimilation of stratospheric chemical tracer observations using a~Kalman filter, Part 2: 2-validated results and analysis of variance and correlation dynamics, Mon. Weather Rev., 128, 2672--2686, 2000.

¥bibitem{91}
Migliorini, S.: On the Equivalence between Radiance and Retrieval Assimilation. *Mon. Wea. Rev.*, **140**, 258--265. doi: http://dx.doi.org/10.1175/MWR-D-10-05047.1, 2012.

¥bibitem{52S}
Mijling,~B., van~der~A,~R.~J., and Zhang,~Q.: Regional nitrogen oxides emission trends in East Asia observed from space, Atmos. Chem. Phys., 13, 12003--12012, doi:¥href{http://dx.doi.org/10.5194/acp-13-12003-2013}{10.5194/acp-13-12003-2013}, 2013.

¥bibitem{56}
Miyazaki,~K. and Eskes,~H.: Constraints on surface ¥chem{NO_x} emissions by assimilating satellite observations of multiple species, Geophys. Res. Lett., 40, 4745--4750, doi:¥href{http://dx.doi.org/10.1002/grl.50894}{10.1002/grl.50894}, 2013.

¥bibitem{53}
Miyazaki,~K., Patra,~P.~K., Takigawa,~M., Iwasaki,~T., and Nakazawa,~T.: Global-scale transport of carbon dioxide in the troposphere,~J. Geophys. Res., 113, D15301, doi:¥href{http://dx.doi.org/10.1029/2007JD009557}{10.1029/2007JD009557}, 2008.

¥bibitem{54S}

Miyazaki,~K., Eskes,~H.~J., and Sudo,~K.: Global ¥chem{NO_x} emission estimates derived from an assimilation of OMI tropospheric NO$_{2}$ columns, Atmos. Chem. Phys., 12, 2263--2288, doi:¥href{http://dx.doi.org/10.5194/acp-12-2263-2012}{10.5194/acp-12-2263-2012}, 2012a.

¥bibitem{55S}
Miyazaki,~K., Eskes,~H.~J., Sudo,~K., Takigawa,~M., van~Weele,~M., and Boersma,~K.~F.: Simultaneous assimilation of satellite NO$_{2}$, O$_{3}$, CO, and HNO$_{3}$ data for the analysis of tropospheric chemical composition and emissions, Atmos. Chem. Phys., 12, 9545--9579, doi:¥href{http://dx.doi.org/10.5194/acp-12-9545-2012}{10.5194/acp-12-9545-2012}, 2012b.

¥bibitem{57S}
Miyazaki,~K., Eskes,~H.~J., Sudo,~K., and Zhang,~C.: Global lightning ¥chem{NO_x} production estimated by an assimilation of multiple satellite data sets, Atmos. Chem. Phys., 14, 3277--3305, doi:¥href{http://dx.doi.org/10.5194/acp-14-3277-2014}{10.5194/acp-14-3277-2014}, 2014.

¥bibitem{58S}
Naik,~V., Voulgarakis,~A., Fiore,~A.~M., Horowitz,~L.~W., Lamarque,~J.-F., Lin,~M., Prather,~M.~J., Young,~P.~J., Bergmann,~D., Cameron-Smith,~P.~J., Cionni,~I., Collins,~W.~J., Dals{¥o}ren,~S.~B., Doherty,~R., Eyring,~V., Faluvegi,~G., Folberth,~G.~A., Josse,~B., Lee,~Y.~H., MacKenzie,~I.~A., Nagashima,~T., van~Noije,~T.~P.~C., Plummer,~D.~A., Righi,~M., Rumbold,~S.~T., Skeie,~R., Shindell,~D.~T., Stevenson,~D.~S., Strode,~S., Sudo,~K., Szopa,~S., and Zeng,~G.: Preindustrial to present-day changes in

tropospheric hydroxyl radical and methane lifetime from the Atmospheric Chemistry and Climate Model Intercomparison Project (ACCMIP), Atmos. Chem. Phys., 13, 5277--5298, doi:¥href{http://dx.doi.org/10.5194/acp-13-5277-2013}{10.5194/acp-13-5277-2013}, 2013.

¥bibitem{59}
Parrington,~M., Jones,~D.~B.~A., Bowman,~K.~W., Thompson,~A.~M., Tarasick,~D.~W., Merrill,~J., Oltmans,~S.~J., Leblanc,~T., Witte,~J.~C., and Millet,~D.~B.: Impact of the assimilation of ozone from the Tropospheric Emission Spectrometer on surface ozone across North America, Geophys. Res. Lett., 36, L04802, ¥doi{10.1029/2008GL036935}, 2009.

¥bibitem{60}
Patra,~P.~K., Krol,~M.~C., Montzka,~S.~A., Arnold,~T., Atlas,~E.~L., Lintner,~B.~R., Stephens,~B.~B., Xiang,~B., Elkins,~J.~W., Fraser,~P.~J., Ghosh,~A., Hintsa,~E.~J., Hurst,~D.~F., Ishijima,~K., Krummel,~P.~B., Miller,~B.~R., Miyazaki,~K., Moore,~F.~L., Mhle,~J., O'Doherty,~S., Prinn,~R.~G., Steele,~L.~P., Takigawa,~M., Wang,~H.~J., Weiss,~R.~F., Wofsy,~S.~C., and Young,~D.: Observational evidence for interhemispheric hydroxyl parity, Nature, 513, 219--223, 2014.

¥bibitem{61}
Petzold,~A., Volz-Thomas,~A., Thouret,~V., Cammas,~J.-P., and Brenninkmeijer,~C.~A.~M.: IAGOS -- In-Service Aircraft for a~Global Observing System, in: 3rd International Conferene on Transport, Atmosphere and Climate, Prien am Chiemsee, Germany, 25--28 June~2012, 69--76, 2013.

¥bibitem{62}
Price,~C. and Rind,~D.: A~simple lightning parameterization for calculating

global lightning distributions,~J. Geophys. Res., 97, 9919--9933, doi:¥href{http://dx.doi.org/10.1029/92JD00719}{10.1029/92JD00719}, 1992.

¥bibitem{63}
Reuter,~M., Buchwitz,~M., Hilboll,~A., Richter,~A., Schneising,~O., Hilker,~M., Heymann,~J., Bovensmann,~H., and Burrows,~J.~P.: Decreasing emissions of ¥chem{NO_x} relative to ¥chem{CO_2} in East Asia inferred from satellite observations, Nat. Geosci., 7, 792--795, doi:¥href{http://dx.doi.org/10.1038/ngeo2257}{10.1038/ngeo2257}, 2014.

¥bibitem{64S}
Schumann,~U. and Huntrieser,~H.: The global lightning-induced nitrogen oxides source, Atmos. Chem. Phys., 7, 3823--3907, doi:¥href{http://dx.doi.org/10.5194/acp-7-3823-2007}{10.5194/acp-7-3823-2007}, 2007.

¥bibitem{68}
Shindell,~D.~T., Faluvegi,~G., Stevenson,~D.~S., Krol,~M.~C., Emmons,~L.~K., Lamarque,~J.-F., Petron,~G., Dentener,~F.~J., Ellingsen,~K., Schultz,~M.~G., Wild,~O., Amann,~M., Atherton,~C.~S., Bergmann,~D.~J., Bey,~I., Butler,~T., Cofala,~J., Collins,~W.~J., Derwent,~R.~G., Doherty,~R.~M., Drevet,~J., Eskes,~H.~J., Fiore,~A.~M., Gauss,~M., Hauglustaine,~D.~A., Horowitz,~L.~W., Isaksen,~I.~S.~A., Lawrence,~M.~G., Montanaro,~V., Mueller,~J.-F., Pitari,~G., Prather,~M.~J., Pyle,~J.~A., Rast,~S., Rodriguez,~J.~M., Sanderson,~M.~G., Savage,~N.~H., Strahan,~S.~E., Sudo,~K., Szopa,~S., Unger,~N., van Noije,~T.~P.~C., and Zeng,~G.: Multimodel simulations of carbon monoxide: comparison with observations and projected near-future changes,~J.~Geophys. Res., 111, D19306, ¥doi{10.1029/2006JD007100}, 2006.

¥bibitem{69S}
Singh,~H.~B., Brune,~W.~H., Crawford,~J.~H., Flocke,~F., and Jacob,~D.~J.:

Chemistry and transport of pollution over the Gulf of Mexico and the Pacific: spring 2006 INTEX-B campaign overview and first results, Atmos. Chem. Phys., 9, 2301--2318, doi:¥href{http://dx.doi.org/10.5194/acp-9-2301-2009}{10.5194/acp-9-2301-2009}, 2009.

¥bibitem{70}
Smit,~H.~G.~J., Straeter,~W., Johnson,~B.~J., Oltmans,~S.~J., Davies,~J., Tarasick,~D.~W., Hoegger,~B., Stubi,~R., Schmidlin,~F.~J., Northam,~T., Thompson,~A.~M., Witte,~J.~C., Boyd,~I., and Posny,~F.: Assessment of the performance of ECC ozonesondes under quasi flight conditions in the environmental simulation chamber: insights from the Juelich Ozone Sonde Intercomparison Experiment (JOSIE),~J. Geophys. Res., 112, D19306, doi:¥href{http://dx.doi.org/10.1029/2006JD007308}{10.1029/2006JD007308}, 2007.

¥bibitem{66}
Stajner,~I. and Wargan,~K.: Antarctic stratospheric ozone from the assimilation of occultation data, Geophys. Res. Lett., 31, L18108, doi:¥href{http://dx.doi.org/10.1029/2004GL020846}{10.1029/2004GL020846}, 2004.

¥bibitem{65}
Stajner,~I., Wargan,~K., Pawson,~S., Hayashi,~H., Chang,~L.~P., Hudman,~R.~C., Froidevaux,~L., Livesey,~N., Levelt,~P.~F., Thompson,~A.~M., Tarasick,~D.~W., St¥"{u}bi,~R., Andersen,~S.~B., Yela,~M., K¥"{o}nig-Langlo,~G., Schmidlin,~F.~J., and Witte,~J.~C.: Assimilated ozone from EOS-Aura: evaluation of the tropopause region and tropospheric columns,~J.~Geophys. Res., 113, D16S32, ¥doi{10.1029/2007JD008863}, 2008.

¥bibitem{67S}

Stein,~O., Schultz,~M.~G., Bouarar,~I., Clark,~H., Huijnen,~V., Gaudel,~A., George,~M., and Clerbaux,~C.: On the wintertime low bias of Northern Hemisphere carbon monoxide found in global model simulations, Atmos. Chem. Phys., 14, 9295--9316, doi:¥href{http://dx.doi.org/10.5194/acp-14-9295-2014}{10.5194/acp-14-9295-2014}, 2014.

¥bibitem{91}
Stone, D., Whalley, L. K., Heard, D. E.: Tropospheric ¥chem{OH} and ¥chem{HO_2} radicals: field measurements and model comparisons.. *Chemical Society Reviews*, 41 (19), 6348-6404, 2012.

¥bibitem{71}
Streets,~D.~G., Bond,~T.~C., Carmichael,~G.~R., Fernandes,~S.~D., Fu,~Q., He,~D., Klimont,~Z., Nelson,~S.~M., Tsai,~N.~Y., Wang,~M.~Q., Woo,~J.~H., and Yarber,~K.~F.: An inventory of gaseous and primary aerosol emissions in Asia in the year 2000,~J. Geophys. Res., 108, 8809, doi:¥href{http://dx.doi.org/10.1029/2002JD003093}{10.1029/2002JD003093}, 2003.

¥bibitem{72}
Streets,~D.~G., Canty,~T., Carmichael,~G.~R., de Foy,~B., Dickerson,~R.~R., Duncan,~B.~N., Edwards,~D.~P., Haynes,~J.~A., Henze,~D.~K., Houyoux,~M.~R., Jacob,~D.~J., Krotkov,~N.~A., Lamsal,~L.~N., Liu,~Y., Lu,~Z., Martin,~R.~V., Pfister,~G., Pinder,~R.~W., Salawitch,~R.~J., and Wecht,~K.~J.: Emissions estimation from satellite retrievals: a~review of current capability, Atmos. Environ., 77, 1011--1042, doi:¥href{http://dx.doi.org/10.1016/j.atmosenv.2013.05.051}{10.1016/j.atmosenv.2013.05.051}, 2013.

¥bibitem{74}
Sudo,~K. and Akimoto,~H.: Global source attribution of tropospheric ozone: long-range transport from various source regions,~J. Geophys. Res., 112,

D12302,
doi:¥href{http://dx.doi.org/10.1029/2006JD007992}{10.1029/2006JD007992},
2007.

¥bibitem{73}
Sudo,~K., Takahashi,~M., and Akimoto,~H.: CHASER: a~global chemical model of the troposphere, 2. Model results and evaluation,~J. Geophys. Res., 107, 4586, doi:¥href{http://dx.doi.org/10.1029/2001JD001114}{10.1029/2001JD001114}, 2002.

¥bibitem{75}
Thompson,~A.~M.: The oxidizing capacity of the Earth's atmossphere: probable past and future changes, Science, 256, 1157--1165, 1992.

¥bibitem{76S}
Thompson,~A.~M., Balashov,~N.~V., Witte,~J.~C., Coetzee,~J.~G.~R., Thouret,~V., and Posny,~F.: Tropospheric ozone increases over the southern Africa region: bellwether for rapid growth in Southern Hemisphere pollution?, Atmos. Chem. Phys., 14, 9855--9869, doi:¥href{http://dx.doi.org/10.5194/acp-14-9855-2014}{10.5194/acp-14-9855-2014}, 2014.

¥bibitem{77S}
van~der~A,~R.~J., Allaart,~M.~A.~F., and Eskes,~H.~J.: Multi sensor reanalysis of total ozone, Atmos. Chem. Phys., 10, 11277--11294, doi:¥href{http://dx.doi.org/10.5194/acp-10-11277-2010}{10.5194/acp-10-11277-2010}, 2010.

¥bibitem{78S}
van~der~Werf,~G.~R., Randerson,~J.~T., Giglio,~L., Collatz,~G.~J., Mu,~M., Kasibhatla,~P.~S., Morton,~D.~C., DeFries,~R.~S., Jin,~Y., and van~Leeuwen,~T.~T.: Global fire emissions and the contribution of deforestation, savanna, forest, agricultural, and peat fires (1997--2009), Atmos. Chem. Phys., 10, 11707--11735, doi:¥href{http://dx.doi.org/10.5194/acp-10-11707-2010}{10.5194/acp-10-11707-2010}, 2010.

¥bibitem{79S}
Verstraeten,~W.~W., Boersma,~K.~F., Z¥"{o}rner,~J., Allaart,~M.~A.~F., Bowman,~K.~W., and Worden,~J.~R.: Validation of six years of TES tropospheric ozone retrievals with ozonesonde measurements: implications for spatial patterns and temporal stability in the bias, Atmos. Meas. Tech., 6, 1413--1423, doi:¥href{http://dx.doi.org/10.5194/amt-6-1413-2013}{10.5194/amt-6-1413-2013}, 2013.

¥bibitem{80}
Wang,~Y., McElroy,~M.~B., Martin,~R.~V., Streets,~D.~G., Zhang,~Q., and Fu,~T.-M.: Seasonal variability of ¥chem{NO_x} emissions over east China constrained by satellite observations: Implications for combustion and microbial sources,~J. Geophys. Res., 112, 1--19, doi:¥href{http://dx.doi.org/10.1029/2006JD007538}{10.1029/2006JD007538}, 2007.

¥bibitem{81}
Wargan,~K., Pawson,~S., Stajner,~I., and Thouret,~V.: Spatial structure of assimilated ozone in the upper troposphere and lower stratosphere,~J. Geophys. Res., 115, D24316,

doi:¥href{http://dx.doi.org/10.1029/2010JD013941}{10.1029/2010JD013941},
2010.

¥bibitem{82S}
Watanabe,~S., Hajima,~T., Sudo,~K., Nagashima,~T., Takemura,~T., Okajima,~H.,
Nozawa,~T., Kawase,~H., Abe,~M., Yokohata,~T., Ise,~T., Sato,~H., Kato,~E.,
Takata,~K., Emori,~S., and Kawamiya,~M.: MIROC-ESM 2010: model description
and basic results of CMIP5-20c3m experiments, Geosci. Model Dev., 4,
845--872,
doi:¥href{http://dx.doi.org/10.5194/gmd-4-845-2011}{10.5194/gmd-4-845-2011},
2011.

¥bibitem{83S}
Wespes,~C., Emmons,~L., Edwards,~D.~P., Hannigan,~J., Hurtmans,~D.,
Saunois,~M., Coheur,~P.-F., Clerbaux,~C., Coffey,~M.~T., Batchelor,~R.~L.,
Lindenmaier,~R., Strong,~K., Weinheimer,~A.~J., Nowak,~J.~B., Ryerson,~T.~B.,
Crounse,~J.~D., and Wennberg,~P.~O.: Analysis of ozone and nitric acid in
spring and summer Arctic pollution using aircraft, ground-based, satellite
observations and MOZART-4 model: source attribution and partitioning, Atmos.
Chem. Phys., 12, 237--259,
doi:¥href{http://dx.doi.org/10.5194/acp-12-237-2012}{10.5194/acp-12-237-2012},
2012.

¥bibitem{84}
Wofsy,~S.~C., Daube,~B.~C., Jimenez,~R., Kort,~E., Pittman,~J.~V., Park,~S.,
Commane,~R., Xiang,~B., Santoni,~G., Jacob,~D., Fisher,~J.,
Pickett-Heaps,~C., Wang,~H., Wecht,~K., Wang,~Q.-Q., Stephens,~B.~B.,
Shertz,~S., Watt,~A.~S., Romashkin,~P., Campos,~T., Haggerty,~J.,
Cooper,~W.~A., Rogers,~D., Beaton,~S., Hendershot,~R., Elkins,~J.~W.,
Fahey,~D.~W., Gao,~R.~S., Moore,~F., Montzka,~S.~A., Schwarz,~J.~P.,

Perring,~A.~E., Hurst,~D., Miller,~B.~R., Sweeney,~C., Oltmans,~S., Nance,~D., Hintsa,~E., Dutton,~G., Watts,~L.~A., Spackman,~J.~R., Rosenlof,~K.~H., Ray,~E.~A., Hall,~B., Zondlo,~M.~A., Diao,~M., Keeling,~R., Bent,~J., Atlas,~E.~L., Lueb,~R., and Mahoney,~M.~J.: HIPPO Merged 10-second Meteorology, Atmospheric Chemistry, Aerosol Data (R¥_20121129). Carbon Dioxide Information Analysis Center, Oak Ridge National Laboratory, Oak Ridge, TN, USA, doi:¥href{http://dx.doi.org/10.3334/CDIAC/hippo_010}{10.3334/CDIAC/hippo¥_010}, (Release 20121129), 2012.

¥bibitem{85S}
Worden,~H.~M., Deeter,~M.~N., Frankenberg,~C., George,~M., Nichitiu,~F., Worden,~J., Aben,~I., Bowman,~K.~W., Clerbaux,~C., Coheur,~P.~F., de~Laat,~A.~T.~J., Detweiler,~R., Drummond,~J.~R., Edwards,~D.~P., Gille,~J.~C., Hurtmans,~D., Luo,~M., Mart¥'{¥i}nez-Alonso,~S., Massie,~S., Pfister,~G., and Warner,~J.~X.: Decadal record of satellite carbon monoxide observations, Atmos. Chem. Phys., 13, 837--850, doi:¥href{http://dx.doi.org/10.5194/acp-13-837-2013}{10.5194/acp-13-837-2013}, 2013.

¥bibitem{86}
Worden,~J., Kulawik,~S.~S., Shephard,~M.~W., Clough,~S.~A., Worden,~H., Bowman,~K., and Goldman,~A.: Predicted errors of tropospheric emission spectrometer nadir retrievals from spectral window selection,~J. Geophys. Res., 109, D09308, doi:¥href{http://dx.doi.org/10.1029/2004JD004522}{10.1029/2004JD004522}, 2004.

¥bibitem{87}
Xiao,~X., Cohan,~D.~S., Byun,~D.~W., and Ngan,~F.: Highly nonlinear ozone formation in the Houston region and implications for emission controls,~J. Geophys. Res., 115, D23309,

doi:¥href{http://dx.doi.org/10.1029/2010JD014435}{10.1029/2010JD014435},
2010.

¥bibitem{88S}
Zbinden,~R.~M., Thouret,~V., Ricaud,~P., Carminati,~F., Cammas,~J.-P., and
N¥'{e}d¥'{e}lec,~P.: Climatology of pure tropospheric profiles and column
contents of ozone and carbon monoxide using MOZAIC in the mid-northern
latitudes (24{¥degree}¥,N to 50{¥degree}¥,N) from 1994 to 2009, Atmos. Chem.
Phys., 13, 12363--12388,
doi:¥href{http://dx.doi.org/10.5194/acp-13-12363-2013}{10.5194/acp-13-12363-2013},
2013.

¥bibitem{89}
Zoogman,~P., Jacob,~D.~J., Chance,~K., Worden,~H.~M., Edwards,~D.~P., and
Zhang,~L.: Improved monitoring of surface ozone air quality by joint
assimilation of geostationary satellite observations of ozone and CO, Atmos.
Environ., 84, 254--261, 2014.

¥end{thebibliography}

¥begin{table}%T1
¥caption{Model minus observation comparisons of the mean ¥chem{O_3} concentrations between the analysis or control run (in brackets) and the observations. The units of the root-mean-square error (RMSE) and bias are ppb. Results are provided for WOUDC ozonesonde observations during 2005--2012, MOZAIC/IAGOS aircraft measurements during 2005--2012, and HIPPO aircraft measurements during 2009--2011.}
¥scalebox{.70}[.70] {¥begin{tabular}{lcccrccrccrccrcc} ¥tophline
&&¥multicolumn{2}{c}{90--55{¥degree}¥,S} &&¥multicolumn{2}{c}{55--15{¥degree}¥,S}
&&¥multicolumn{2}{c}{15S--15{¥degree}¥,N} &&¥multicolumn{2}{c}{15--55{¥degree}¥,N}
&&¥multicolumn{2}{c}{55--90{¥degree}¥,N} ¥¥

¥cline{3-4} ¥cline{6-7} ¥cline{9-10} ¥cline{12-13} ¥cline{15-16}
&&Bias &RMSE &&Bias &RMSE& &Bias &RMSE &&Bias &RMSE &&Bias &RMSE ¥¥
¥middlehline
&850-- &$-$1.7 &4.0 &&$-$1.0 &5.6& &2.8 &7.4 &&$-$0.9 &6.9 &&$-$3.9 &6.0 ¥¥
&500 & ($-$1.6) &(4.2) && ($-$1.2) &(6.0) &&(0.6) &(7.4) && ($-$2.4) &(7.3) && ($-$5.4) &(6.5) ¥¥
WOUDC &500-- &5.0 &19.6 &&$-$1.9 &14.6 &&1.0 &9.4 &&$-$1.3 &17.7& &$-$8.0 &29.0 ¥¥
sonde &200 &(32.5) &(32.7) &&(11.5) &(21.5) && ($-$2.6) &(10.0) && ($-$0.2) &(19.1) && ($-$12.3) &(31.7) ¥¥
&200-- &46.3 &88.8 &&7.6 &48.7 &&$-$1.6 &19.7& &4.0 &67.1 &&2.7 &95.2 ¥¥
&90 &(240.4) &(202.8) &&(103.7) &(100.6) &&(4.0) &(25.3) &&(44.3) &(84.1) &&(34.8) &(125.4) ¥¥
¥hhline
&850-- &-- &-- &&-- &--& &4.1 &11.2 &&2.7 &10.3 &&$-$1.7 &8.1 ¥¥
&500 &-- &-- &&-- &-- &&(1.6) &(11.0) &&(1.0) &(10.3) && ($-$3.9) &(8.8) ¥¥
MOZAIC/IAGOS &500-- &-- &-- &&-- &-- &&4.2 &11.4 &&4.8 &16.3 &&$-$2.7 &36.5 ¥¥
aircraft &300 &-- &-- &&-- &-- &&(0.6) &(11.8) &&(4.8) &(16.9) && ($-$2.8) &(37.1) ¥¥
&300-- &-- &-- &&-- &-- &&6.8 &14.2 &&6.1 &34.1 &&7.3 &64.0 ¥¥
&200 &-- &-- &&-- &-- && ($-$0.3) &(13.9) &&(7.2) &(36.7) && ($-$17.6) &(69.4) ¥¥
¥hhline
&850-- &0.1 &6.1 &&1.0 &6.9 &&2.3 &8.4 &&$-$0.9 &10.0 &&$-$3.1&7.5 ¥¥
HIPPO &500 &(0.9) &(6.6) &&(1.4) &(7.4)& &(1.3) &(8.3) && ($-$2.6) &(10.3) && ($-$5.3) &(8.1) ¥¥
aircraft &500-- &$-$3.5 &28.1 &&4.2 &15.2 &&4.2 &10.2 &&3.5 &20.8& &$-$2.2 &42.9 ¥¥
&200 &(33.8) &(46.4) &&(15.3) &(23.3) &&(3.1) &(10.7) &&(4.0) &(22.8) && ($-$4.1) &(46.3) ¥¥
¥bottomhline
¥end{tabular}}
¥end{table}

¥begin{table}
¥caption{Linear trend (slope in ¥unit{ppb¥,(8¥,years)^{-1}}) and standard deviation (in ¥unit{ppb}) of ¥chem{O_3} derived from the WMO ozonesonde observations, the control run, and the reanalysis during 2005--2012.}
¥scalebox{.55}[.55] {¥begin{tabular}{lccrccrccrccrcc} ¥tophline

```
 &¥multicolumn{2}{c}{90--55{¥degree}¥,S}  &&¥multicolumn{2}{c}{55--15{¥degree}¥,S}
&&¥multicolumn{2}{c}{15S--15{¥degree}¥,N}  &&¥multicolumn{2}{c}{15--55{¥degree}¥,N}
&&¥multicolumn{2}{c}{55--90{¥degree}¥,N} ¥¥
¥cline{2-3} ¥cline{5-6} ¥cline{8-9} ¥cline{11-12} ¥cline{14-15}
 &Obs &Reanalysis &&Obs &Reanalysis &&Obs &Reanalysis &&Obs &Reanalysis &&Obs &Reanalysis ¥¥
 &&(Control) &&&(Control) &&&(Control) &&&(Control) &&&(Control) ¥¥
¥middlehline
850-- &$- 0.2 ¥pm 2.9$  &$- 0.8 ¥pm 2.7$  &&$+2.4 ¥pm 2.9$  &$- 0.5 ¥pm 3.0$  &&$- 6.3 ¥pm 2.3$  &$- 1.6 ¥pm 1.7$  &&$+2.9 ¥pm 2.8$  &$+1.2 ¥pm 2.1$ & &$+1.1 ¥pm 2.4$  &$+1.8 ¥pm 1.8$  ¥¥
500 &&($+0.2 ¥pm 2.6$) &&&($-0.7 ¥pm 3.1$) &&&($-1.8 ¥pm 1.4$) &&&($-1.2 ¥pm 2.1$) &&&($+0.2 ¥pm 1.9$) ¥¥
500-- &$- 2.5 ¥pm 5.5$  &$+8.2 ¥pm 4.1$  &&$+7.7 ¥pm 5.7$  &$+7.2 ¥pm 5.3$  &&$- 1.8 ¥pm 3.0$  &$- 0.9 ¥pm 2.0$  &&$+1.1 ¥pm 7.9$  &$- 0.3 ¥pm 7.1$  &&$- 7.1 ¥pm 17.1$  &$- 4.2 ¥pm 15.4$  ¥¥
 200 &&($-1.4 ¥pm 6.9$) &&&($+0.9 ¥pm 6.4$) &&&($-1.7 ¥pm 1.5$) &&&($-3.8 ¥pm 7.1$) &&&($-3.1 ¥pm 14.9$) ¥¥
200-- &$- 13.6 ¥pm 36.7$  &$- 1.2 ¥pm 36.7$  &&$+7.2 ¥pm 29.5$  &$+3.3 ¥pm 29.7$ & &$+3.8 ¥pm 7.5$  &$+0.7 ¥pm 6.9$  &&$- 17.7 ¥pm 41.9$  &$- 25.7 ¥pm 38.8$ & &$- 67.7 ¥pm 78.4$  &$- 72.7 ¥pm 74.9$  ¥¥
 90 &&($-4.4 ¥pm 36.4$) &&&($-6.5 ¥pm 33.1$) &&&($-1.7 ¥pm 6.4$) &&&($-35.8 ¥pm 46.3$) &&&($-68.0 ¥pm 85.6$) ¥¥
¥bottomhline
¥end{tabular}}
¥end{table}

¥begin{table}
¥caption{Comparisons of the mean ¥chem{O_3} concentrations between the
reanalysis run and the WOUDC ozonesonde observations in the SH
(90--30{¥degree}¥,S), TR (30{¥degree}¥,S--30{¥degree}¥,N) and NH
(30--90{¥degree}¥,N). The mean differences are shown for each year of the
reanalysis period and for mean concentrations during 2005--2009 and during
2010--2012. The latter includes results for the control run given in
brackets.} ¥scalebox{.95}[.95] {¥begin{tabular}{lcccrcccrccc} ¥tophline
```

```
&¥multicolumn{3}{c}{850--500}                    &&¥multicolumn{3}{c}{500--200}
&&¥multicolumn{3}{c}{200--90}    ¥¥
¥cline{2-4} ¥cline{6-8} ¥cline{10-12}
&SH &TR &NH &&SH &TR &NH    &&SH &TR &NH    ¥¥
¥middlehline
2005 &$-$2.3 &0.9 &$-$2.3 &&3.0 &0.4 &0.9 &&27.3 &4.6 &13.3 ¥¥
2006 &$-$0.2 &1.1 &$-$2.6 &&0.2 &$-$0.3 &$-$4.9 &&27.3 &$-$2.7 &3.9 ¥¥
2007 &0.2 &0.8 &$-$2.5 &&$-$2.1 &$-$0.6 &$-$5.4 &&23.8 &$-$1.9 &$-$1.3 ¥¥
2008 &1.4 &1.9 &$-$1.8 &&0.7 &1.2 &$-$5.2 &&30.9 &1.2 &10.8 ¥¥
2009 &0.2 &2.3 &$-$2.0 &&2.7 &0.3 &$-$8.4 &&33.6 &$-$3.1 &3.2 ¥¥
2010 &$-$2.5 &3.5 &$-$2.8 &&7.1 &0.7 &$-$6.6 &&42.8 &1.4 &$-$5.3 ¥¥
2011 &$-$2.3 &1.8 &$-$2.7 &&7.1 &0.3 &$-$3.7 &&30.8 &$-$6.4 &$-$2.5 ¥¥
2012 &$-$1.9 &2.0 &$-$3.6 &&6.8 &$-$1.6 &2.9 &&31.5 &$-$5.1 &10.1 ¥¥
¥hhline
2005--2009 &$-$0.1 &1.4 &$-$2.2 &&0.9 &0.2 &$-$4.6 &&28.6 &$-$0.4 &6.0 ¥¥
  & ($-$0.3) & ($-$0.3) & ($-$3.5) &&(27.6) & ($-$2.2) & ($-$3.0) &&(193.8) &(11.0) &(52.0) ¥¥
2010--2012 &$-$2.3 &2.4 &$-$3.0 &&7.0 &$-$0.2 &$-$2.5 &&35.0 &$-$3.4 &0.8 ¥¥
  & ($-$1.2) & ($-$0.6) & ($-$5.6) &&(26.5) & ($-$3.2) & ($-$4.7) &&(191.0) &(6.5) &(45.9) ¥¥
¥bottomhline
¥end{tabular}}
¥end{table}

¥begin{table}
¥caption{Same as Table~1, but for mean ¥chem{CO} concentrations. The unit is
ppb. Observations used are the WDCGG observations during 2005--2012,
MOZAIC/IAGOS aircraft measurements during 2005--2012, and HIPPO aircraft
measurements during 2009--2011.} ¥scalebox{.70}[.70]
{¥begin{tabular}{lcccrccrccrccrcc} ¥tophline
&&¥multicolumn{2}{c}{90--55{¥degree}¥,S}        &&¥multicolumn{2}{c}{55--15{¥degree}¥,S}
&&¥multicolumn{2}{c}{15S--15{¥degree}¥,N}      &&¥multicolumn{2}{c}{15--55{¥degree}¥,N}
&&¥multicolumn{2}{c}{55--90{¥degree}¥,N} ¥¥
¥cline{3-4}¥cline{6-7}¥cline{9-10}¥cline{12-13}¥cline{15-16}
&&Bias &RMSE &&Bias &RMSE &&Bias &RMSE &&Bias &RMSE &&Bias &RMSE ¥¥
¥middlehline
WDCGG &&$-$0.6 &7.3 &&4.3 &19.8& &$-$13.6 &27.4 &&27.2 &62.8 &&11.1 &40.0 ¥¥
```

surface && ($-$4.6) &(8.0) && ($-$5.8) &(15.8) && ($-$18.9) &(33.4) && ($-$41.7) &(60.4) && ($-$51.1) &(57.9) ¥¥
¥hhline
&850-- &-- &-- &&-- &--& &$-$19.8 &34.6 &&$-$15.1 &29.3& &$-$10.5 &15.6 ¥¥
&500 &-- &-- &&-- &-- && ($-$37.7) &(45.6) && ($-$48.3) &(53.1) && ($-$51.1) &(51.5) ¥¥
MOZAIC/IAGOS &500-- &-- &--& &-- &-- &&$-$10.3 &18.1 &&$-$8.6 &18.9& &$-$3.4 &19.7 ¥¥
aircraft &300 &-- &-- &&-- &-- && ($-$21.3) &(25.4) && ($-$30.0) &(33.6) && ($-$30.9) &(35.3) ¥¥
&300-- &-- &-- &&-- &-- &&$-$9.9 &24.4 &&0.0 &18.2 &&10.2 &23.5 ¥¥
&200 &-- &-- &&-- &-- && ($-$21.5) &(30.6) & &($-$16.8) &(24.7) && ($-$10.0) &(24.8) ¥¥
¥hhline
&850-- &2.1 &2.8 &&$-$0.6 &5.1 &&$-$3.6 &6.9 &&$-$11.8 &17.1 &&$-$11.5 &16.4 ¥¥
HIPPO &500 & ($-$1.6) &(2.4) && ($-$4.8) &(5.9) && ($-$8.8) &(10.6) && ($-$35.3) &(37.0) && ($-$49.5) &(50.0) ¥¥
aircraft &500-- &6.2 &7.4 &&$-$1.2 &6.7& &$-$2.0 &6.7 &&$-$7.2 &17.0 &&$-$4.3 &23.7 ¥¥
&200 &(2.6) &(6.5) & &($-$5.0) &(7.8) && ($-$7.0) &(9.0) && ($-$23.9) &(28.4) && ($-$27.9) &(38.1) ¥¥
¥bottomhline
¥end{tabular}}
¥end{table}

¥begin{table}
¥caption{Comparisons of global tropospheric ¥chem{NO_2} columns between the control run and the satellite retrievals in brackets, and between the reanalysis run and the satellite retrievals: OMI for 2005--2012, SCIAMACHY for 2005--2011, and GOME-2 for 2007--2012. The bias represents the control run or reanalysis minus the retrievals. The AK of each retrieval is applied to the control run and the reanalysis. The units for the RMSE and bias are 10^{15}¥,¥unit{molec¥,cm^{-2}}.}
¥begin{tabular}{lcccc}
¥tophline
&OMI &SCIAMACHY &GOME-2 ¥¥
¥middlehline
S-Corr &0.970 &0.916 &0.924 ¥¥
&(0.931) &(0.862) &(0.881) ¥¥
¥cline{1-4}

BIAS &$-$0.048 &$-$0.091 &$-$0.185 ¥¥
& ($-$0.122) & ($-$0.162) & ($-$0.256) ¥¥
¥cline{1-4}
RMSE &0.383 &0.946 &0.847 ¥¥
&(0.533) &(1.102) &(0.990) ¥¥
¥bottomhline
¥end{tabular}
¥end{table}

¥begin{table}
¥caption{Model minus observation ~~Comparison~~ comparison of mean ¥chem{O_3} concentrations (in ppb) between the control/reanalysis calculations and the ozonesonde observations for 2005 in the SH (90--30{¥degree}¥,S), TR (30{¥degree}¥,S--30{¥degree}¥,N) and NH (30--90{¥degree}¥,N). Sensitivity reanalysis calculations were conducted by excluding the emission factors from the state vector (w/o emission), with TES ¥chem{O_3} bias correction (TES-bias), without assimilation of TES measurements (w/o TES), and with HTAP-v2 emission inventories for 2008 as the a~priori surface emissions (HTAP).}
%¥scalebox{.85}[.85]
{¥begin{tabular}{lcccrcccrccc} ¥tophline
&¥multicolumn{3}{c}{850--500} &&¥multicolumn{3}{c}{500--200}
&&¥multicolumn{3}{c}{200--90} ¥¥
¥cline{2-4} ¥cline{6-8} ¥cline{10-12}
&SH &TR &NH &&SH &TR &NH &&SH &TR &NH ¥¥
¥middlehline
Control &$-$0.8 &$-$0.6 &$-$3.5& &27.9 &$-$2.3 &$-$1.4 &&195.9 &18.0 &72.1 ¥¥
Reanalysis &$-$2.3 &1.0 &$-$2.3 &&3.0 &0.4 &0.9 &&27.3 &4.6 &13.2 ¥¥
w/o emission &$-$3.2 &$-$0.5 &$-$3.2 &&2.3 &$-$1.7 &$-$0.7 &&28.5 &3.6 &14.3 ¥¥
TES-bias &$-$4.4 &$-$0.1 &$-$4.9 &&0.7 &$-$0.4 &$-$2.7 &&25.4 &4.8 &13.2 ¥¥
w/o TES &$-$1.1 &1.7 &$-$1.0 &&9.3 &1.6 &5.6 &&27.5 &5.7 &14.6 ¥¥
HTAP &$-$1.9 &1.9 &0.1 &&3.1 &0.7 &2.1 &&28.4 &8.3 &16.3 ¥¥
¥bottomhline
¥end{tabular}}
¥end{table}

¥begin{figure}

¥includegraphics[width=40mm]{acp-2015-127-discussions-f01.pdf}
¥caption{Time series of the monthly mean Chi-square value and its
standard deviation (black lines) and the number of assimilated
observations per month (blue bars) for OMI ¥chem{NO_2}, TES
¥chem{O_3}, MOPITT ¥chem{CO}, MLS ¥chem{O_3}, and MLS
¥chem{HNO_3}. A~super-observation approach is employed to the OMI
and MOPITT measurements (the number of the super observation is
shown), whereas individual observations are used in the analysis of
the others.}
¥end{figure}

¥begin{figure}
¥includegraphics[width=110mm]{acp-2015-127-discussions-f02.pdf}
¥caption{Time--latitude cross-section of the monthly and zonal mean
OmF obtained without assimilation (left panels) and with
assimilation (centre panels). The positive and negative OmF values
are shown in red and blue, respectively. Positive OmF represents
negative model bias compared with observations. Right panels show
latitudinal distributions of the eight-year mean OmF bias (black
line) and RMSE (red line) obtained with assimilation (solid line)
and without assimilation (dotted line). The 1st row is the OmF for
OMI ¥chem{NO_2} data (in 10^{15}¥,¥unit{molec¥,cm^{-2}}); 2nd row
for TES ¥chem{O_3} data between 500 and 300¥,¥unit{hPa} (in
¥unit{ppb}); 3rd row for MOPITT ¥chem{CO} data between 700 and
500¥,¥unit{hPa} (in ¥unit{ppb}); 4th row for MLS ¥chem{O_3} data
between 216 and 100¥,¥unit{hPa} (in ¥unit{~~ppb~~ppm}); and 5th row for MLS
¥chem{HNO_3} data between 150 and 80¥,¥unit{hPa} (in
¥unit{ppb}). A~super-observation approach is employed to the OMI and
MOPITT measurements, whereas individual observations are used in the
analysis of the others.}
¥end{figure}

¥begin{figure}
¥includegraphics[width=130mm]{acp-2015-127-discussions-f03.pdf}

¥caption{Time--latitude cross section of the analysis increment (upper
panels, in ppb/analysis step) and the analysis spread (lower panels, in ppb/analysis step)
obtained for ¥chem{O_3} at 700¥,¥unit{hPa} (left), 400¥,¥unit{hPa}
(centre), and 200¥,¥unit{hPa} (right).}
¥end{figure}

¥begin{figure}
¥includegraphics[width=60mm]{acp-2015-127-discussions-f04.pdf}
¥caption{Comparison of the vertical ¥chem{O_3} profiles between
ozonesondes (black), control run (blue), and reanalysis (red)
averaged for the period 2005--2012. The left column shows the mean
profile; centre and right columns show the mean difference and the
RMSE between the control run and the observations (blue) and between
the reanalysis and the observations (red). From top to bottom,
results are shown for the NH high latitudes (55--90{¥degree}¥,N), NH
mid latitudes (15--55{¥degree}¥,N), tropics
(15{¥degree}¥,S--15{¥degree}¥,N), SH mid latitudes
(15--55{¥degree}¥,S), and SH high latitudes (55--90{¥degree}¥,S).}
¥end{figure}

¥begin{figure}
¥includegraphics[width=100mm]{acp-2015-127-discussions-f05.pdf}
¥caption{Time series of the monthly mean ¥chem{O_3} concentration
obtained from ozonesondes (black), control run (blue), and
reanalysis (red) averaged between 850--500¥,¥unit{hPa} (left
column), 500--200¥,¥unit{hPa} (center column), and
200--90¥,¥unit{hPa} (right column). From top to bottom the results
are shown for the NH high latitudes (55--90{¥degree}¥,N), NH
mid-latitudes (15--55{¥degree}¥,N), tropics
(15{¥degree}¥,S--15{¥degree}¥,N), SH mid-latitudes
(15--55{¥degree}¥,S), and SH high latitudes (55--90{¥degree}¥,S).}
¥end{figure}

¥begin{figure}
¥includegraphics[width=90mm]{acp-2015-127-discussions-f06.pdf}

¥caption{Vertical profiles of the time series of the monthly mean ¥chem{O_3} concentration difference (in {¥%}) between the control run and ozonesondes (top) and between the reanalysis and ozonesondes (bottom) averaged over the NH mid-latitudes (15--55{¥degree}¥,N).}
¥end{figure}

¥begin{figure}
¥includegraphics[width=80mm]{acp-2015-127-discussions-f07.pdf}
¥caption{Spatial distributions of ¥chem{O_3} (left column) and ¥chem{CO} (right column) averaged between 500 and 300¥,¥unit{hPa} and during 2005--2012 obtained from the MOZAIC/IAGOS aircraft measurements (1st row), control run (2nd row), and reanalysis (3rd row). Difference between the control run and observations (4th row) and between the reanalysis and observations (5th row) are also plotted. Units are ¥unit{ppb}.}
¥end{figure}

¥begin{figure}
¥includegraphics[width=120mm]{acp-2015-127-discussions-f08.pdf}
¥caption{Time series of the monthly mean ¥chem{O_3} concentration obtained from the MOZAIC/IAGOS aircraft measurements (black), control run (blue), and reanalysis (red) averaged between 850--500¥,¥unit{hPa} (left column), 500--300¥,¥unit{hPa} (centre column), and 300--200¥,¥unit{hPa} (right column). From top to bottom the results are shown for the NH high latitudes (55--90{¥degree}¥,N), NH mid-latitudes (15--55{¥degree}¥,N), and tropics (15{¥degree}¥,S--15{¥degree}¥,N).}
¥end{figure}

¥begin{figure}
¥includegraphics[width=130mm]{acp-2015-127-discussions-f09.~~pdf~~eps}
¥caption{Latitude--pressure cross section of mean ¥chem{O_3} concentration (in ¥unit{ppb}) obtained from HIPPO aircraft measurements (1st row), control run (2nd row), and reanalysis (3rd row). The relative difference (in ¥%) between the control run and the observation (4th row) and

between the reanalysis and the observation (5th row) is also shown. Results are shown for all HIPPO campaigns (HIPPO I, 8--30
January~2009; HIPPO II, 31 October to 22 November~2009; HIPPO III, 24 March to 16 April~2010; HIPPO IV, 14 June to 11 July~2011; and HIPPO V, 9 August to 9 September~2011 from left to right).}
¥end{figure}

¥begin{figure}
¥includegraphics[width=130mm]{acp-2015-127-discussions-f10.pdf}
¥caption{Mean vertical profiles of ¥chem{O_3} (¥chem{ppb}), ¥chem{CO} (¥chem{ppb}), ¥chem{NO_2} (¥chem{ppb}), ¥chem{OH} (¥chem{ppt}), ¥chem{HO_2} (¥chem{ppb}), ¥chem{HNO_3} (¥chem{ppt}), and ¥chem{CH_2O} (¥chem{ppt}) obtained from aircraft measurements (black), control run (blue), and reanalysis (red), for the INTEX-B profile (1st row), ARCTAS-A~profile (2nd row), ARCTAS-B profile (3rd row), DISCOVER-AQ profile (4th row), DC3-DC8 profile (5th row), and DC3-GV profile (6th row). Error bars represent the standard deviation of all data within one bin (with an interval of 30¥,¥unit{hPa}).}
¥end{figure}

¥begin{figure}
¥includegraphics[width=120mm]{acp-2015-127-discussions-f11.pdf}
¥caption{Time series of monthly mean ¥chem{CO} concentration obtained from the WDCGG ground measurements (black), control run (blue), and reanalysis (red). Model simulation results with the HTAP emissions are also plotted (green).}
¥end{figure}

¥begin{figure}
¥includegraphics[width=120mm]{acp-2015-127-discussions-f12.pdf}
¥caption{Same as in Fig.~8, but for ¥chem{CO} concentration obtained from MOZAIC/IAGOS aircraft measurements.}
¥end{figure}

¥begin{figure}
¥includegraphics[width=130mm]{acp-2015-127-discussions-f13.~~pdf~~eps}
¥caption{Same as in Fig.~9, but for ¥chem{CO} concentration (in ¥unit{ppb}, fro 1st to 3rd row) and its absolute difference (in ¥unit{ppb}, from 4th to 5th row) obtained from HIPPO aircraft measurements.}
¥end{figure}

¥begin{figure}
¥includegraphics[width=80mm]{acp-2015-127-discussions-f14.pdf}
¥caption{Time series of regional monthly mean tropospheric ¥chem{NO_2} columns (in 10^{15}¥,¥unit{molec¥,cm^{-2}}) averaged over eastern China (110--123{¥degree}¥,E, 30--40{¥degree}¥,N), Europe (10{¥degree}¥,W--30{¥degree}¥,E, 35--60{¥degree}¥,N), the eastern United States (71--95{¥degree}¥,W, 32--43{¥degree}¥,N), Northern Africa (20{¥degree}¥,W--40{¥degree}¥,E, Equator--20{¥degree}¥,N), Central Africa (10--40{¥degree}¥,E, Equator--20{¥degree}¥,S), southeast Asia (96--105{¥degree}¥,E, 10--20{¥degree}¥,N) obtained from the satellite retrievals (black), control run (blue), and reanalysis (red). Results are shown for the OMI retrievals (left columns), SCIAMACHY retrievals (centre columns), and GOME-2 retrievals (right columns).}
¥end{figure}

¥begin{figure}
¥includegraphics[width=70mm]{acp-2015-127-discussions-f15.pdf}
¥caption{Time series of monthly total global and regional surface ¥chem{NO_x} emissions (in ¥unit{Tg¥,N¥,yr^{-1}}, top), ¥chem{LNO_x} emissions (in ¥unit{Tg¥,N¥,yr^{-1}}, centre), and surface ¥chem{CO} emissions (in ¥unit{Tg¥,CO¥,yr^{-1}}, bottom) obtained from the reanalysis (solid lines) and the emission inventories or the control run (dashed lines) over the globe (90{¥degree}¥,S--90{¥degree}¥,N), NH (20--90{¥degree}¥,N), tropics (TR, 20{¥degree}¥,S--20{¥degree}¥,N), and SH (90--20{¥degree}¥,S). The eight-year mean emissions values obtained from the reanalysis run and the emission inventories (in bracket) are shown on the

```
   right-hand side.}
¥end{figure}

¥begin{figure}
¥includegraphics[width=120mm]{acp-2015-127-discussions-f16.png}
¥caption{Global distributions of surface ¥chem{NO_x} emissions (left
   columns), ¥chem{LNO_x} sources (centre columns), and surface
   ¥chem{CO} emissions (right columns) averaged over 2005--2012. The
   a~priori emissions (upper rows), a~posteriori emissions (middle
   rows), and analysis increment (lower rows), i.e., the difference
   between the a~posteriori and the a~priori emissions, are shown for
   each panel.}
¥end{figure}

¥begin{figure}
¥includegraphics[width=80mm]{acp-2015-127-discussions-f17.pdf}
¥caption{Month--pressure cross section of the zonal mean bias of
   ¥chem{O_3} concentration (in {¥%}) compared with the ozonesonde
   observations averaged over 30--60{¥degree} for the reanalysis run
   (top) and the sensitivity experiment that excludes the emission
   factors from the state vector (w/o emission, bottom).}
¥end{figure}

¥begin{figure}
¥includegraphics[width=120mm]{acp-2015-127-discussions-f18.pdf}
¥caption{Latitude--pressure cross section of the eight-year mean
   ¥chem{OH} concentration (right panels) and time-latitude
   cross-section of the monthly mean ¥chem{OH} concentration averaged
   between 1000 and 300¥,¥unit{hPa} (left panels). The ¥chem{OH}
   concentration obtained from the reanalysis (top panels) and the
   difference between the reanalysis and the control run (bottom
   panels) are also shown. Units are ¥unit{ppt}.}
¥end{figure}
```

¥end{document}